

# Automated Digital System Engineering Model

L.G. Hause  
D.R. Wortendyke



**U.S. DEPARTMENT OF COMMERCE**  
**Juanita M. Kreps, Secretary**

Henry Geller, Assistant Secretary  
for Communications and Information

March 1979



## TABLE OF CONTENTS

	Page
ABSTRACT	1
1. INTRODUCTION	1
2. PROGRAM NO. 1, EARTH GEOMETRY AND PROGRAM NO. 2, PATH PROFILE AND RAY-PATH CHARACTERISTICS	7
3. PROGRAM NO. 3, MEDIAN BASIC TRANSMISSION LOSS MODEL	25
4. PROGRAM NO. 4, PATH-LOSS VARIABILITY MODEL	33
5. PROGRAM NO. 5, LINK EQUIPMENT GAIN	51
6. PROGRAM NO. 6, LINK PERFORMANCE CALCULATIONS	59
7. PROGRAM NO. 7, SYSTEM PERFORMANCE	80
8. RECOMMENDATIONS	84
9. REFERENCES	85

## LIST OF FIGURES

Figure 1-1. Diagram for the design of a microwave radio communications system.	3
Figure 1-2. Automated system engineering model.	4
Figure 2-1. Earth geometry model.	9
Figure 2-2. Earth geometry program flow chart.	10
Figure 2-3. Spherical triangle for great-circle path computations.	14
Figure 2-4. Terrain profile and ray-path model.	18
Figure 2-5. Example of terrain profile and ray paths.	19
Figure 3-1. Median basic transmission loss model.	26
Figure 3-2. Mean temperature values (use July values for the Northern Hemisphere and January values for the Southern Hemisphere). (From "Climates of the World", U.S. Dept. of Comm., ESSA, Environmental Data Service, January 1969.)	28

	Page
Figure 3-3. Contours of average absolute humidity ( $\text{g}/\text{m}^3$ ) for a summer month (August for the northern hemisphere and February for the southern hemisphere) (Bean and Dutton, 1966).	30
Figure 4-1. Path-loss variability model.	34
Figure 4-2. Comparison of prediction methods with one year of data from an LOS path across the English Channel (88 km, 5 GHz).	35
Figure 4-3. Example basic transmission loss variability distributions.	38
Figure 4-4. Annual precipitation, $M$ , in millimeters, for an average year in Europe.	41
Figure 4-5. Mean annual thunderstorm ratio, $\beta$ , for Europe. (Dashed contours indicate regions of sparse data.)	42
Figure 4-6. The estimated number of rainy days, $D$ , for an average year in Europe.	43
Figure 4-7. 30-year mean annual precipitation, $M$ , in millimeters, for the U.S.A.	44
Figure 4-8. Mean annual thunderstorm ratio, $\beta$ , for the U.S.A.	45
Figure 4-9. 30-year annual number of days, $D$ , with precipitation greater than 0.25 mm for the U.S.A.	46
Figure 4-10. Mean annual thunderstorm ratio, $\beta$ , for the world.	47
Figure 4-11. Example point rain rate distribution.	48
Figure 5-1. Link equipment gain.	52
Figure 5-2. Microwave waveguide attenuation.	54
Figure 5-3. Time availability of received signal level.	58
Figure 6-1. Link performance evaluation.	60
Figure 6-2. Waveguide velocity curves.	67
Figure 6-3. Maximum distortion to signal ratio due to echo.	69

	Page
Figure 6-4. Example of a worst channel FM-FDM receiver transfer characteristic.	72
Figure 6-5. Example of a digital receiver transfer characteristic.	74
Figure 7-1. System performance evaluation.	81

#### LIST OF TABLES

Table 2-1. Example of an Earth Geometry Tabular Output	11
Table 2-2. Earth Radius For Various Spheroids	12
Table 2-3. Example of Microwave Path Tabulation	20
Table 3-1. Oxygen Lines	29
Table 3-2. Water Vapor Lines	31
Table 3-3. Example of the Tabular Output Format From the Median Basic Transmission Loss Model	32
Table 4-1. Example of Tabular Output of Path Loss Variability Information	39
Table 5-1. Sample Summary of Basic Link and Equipment Gain Parameters	56
Table 6-1. Example of the Link Performance Summary	75
Table 7-1. Example FM/FDM System Performance Table	82
Table 7-2. Example Digital System Performance Table	83



## AUTOMATED DIGITAL SYSTEM ENGINEERING MODEL

L.G. Hause and D.R. Wortendyke\*

This report describes a desk-top computer system and mathematical models which were used in seven of its programs. These programs make key calculations in the design of line-of-sight microwave systems. The models have the following ranges; bit rates up to 50 Mbits/s, carrier frequencies from 1 to 40 GHz, and path distances up to 150 km. The programs calculate, tabulate and plot information about earth geometry, path profiles and ray paths, median basic transmission loss, path-loss variability, equipment gain, link performance, and system performance. Models were chosen based on their wideness of acceptance and the size and type of data base substantiating the model. Any design engineer using this model can have immediate access to calculated results corresponding to changes in design parameters. The reasons for this capability are that the programs are written for use in an interactive mode and the programs can be used by people with no experience in programming.

Key words: Line-of-sight microwave, computer programs, earth geometry, path profiles, basic transmission loss, digital systems, microwave link performance, multipath fading, rain attenuation

### 1. INTRODUCTION

The purpose of this report is to describe a program which developed an interactive automated engineering model used in the design of line-of-sight microwave communications systems. The concept of this engineering model is based in large part on the information and methodology contained in MIL-HDBK-416 (1977) which was prepared by the Institute for Telecommunication Sciences (ITS), under an Air Force contract. The handbook was written several years ago; consequently, emphasis was placed on analog systems (FM/FDM) with little information on digital systems. With the passage of time, many of the original models used to predict path-loss variability and other factors affecting performance have been improved.

---

\*The authors are with the National Telecommunications and Information Administration, Institute for Telecommunication Sciences, U.S. Dept. of Commerce, Boulder, Colorado 80303.

Much emphasis in this program (sponsored by USACC EED-PED) is placed on adding needed models and updating ones which have been improved.

Obviously not all aspects of a line-of-sight system design can be automated and such things as procedures for making a field survey of potential terminal sites are much the same as described in MIL-HDBK-416. These topics were not reexamined during this program. The primary objective for this project is to automate tedious calculations within various models which are compatible with a calculator\* based system operated in a highly interactive mode. This type of operation permits the system design engineer to evaluate many different configurations with immediate feedback in terms of system performance and tradeoffs. Among the benefits from this kind of automation are the time saved when batch processing is not necessary and a more nearly optimum design choice that results from the capability of the system designer to view the results of design changes immediately.

This report discusses three topics:

1. A brief description of the Hewlett-Packard 9825A\*\* calculator system is presented.
2. A block diagram and description is presented of the various stages of the microwave system design (Figure 1-1). The blocks are selected to follow the evolution of the design. A second diagram of the automated system is presented with blocks representing segments of effort that terminate at logical reporting times (Figure 1-2). The second diagram includes only that part of the design which is compatible with the calculator based system.
3. Flow diagrams and descriptions of the various particular models are presented with the reasons why some models were added, others modified, and some left essentially unchanged from their original presentation in MIL-HDBK-416.

---

\*For desk-top computers, the terms calculator and computer have become interchangeable in usage by both manufacturers and government agencies.

\*\*The use of trade names in this volume is necessary since the computer system and language are unique to the manufacturer who provided them. Such use of the trade name does not constitute a product endorsement.

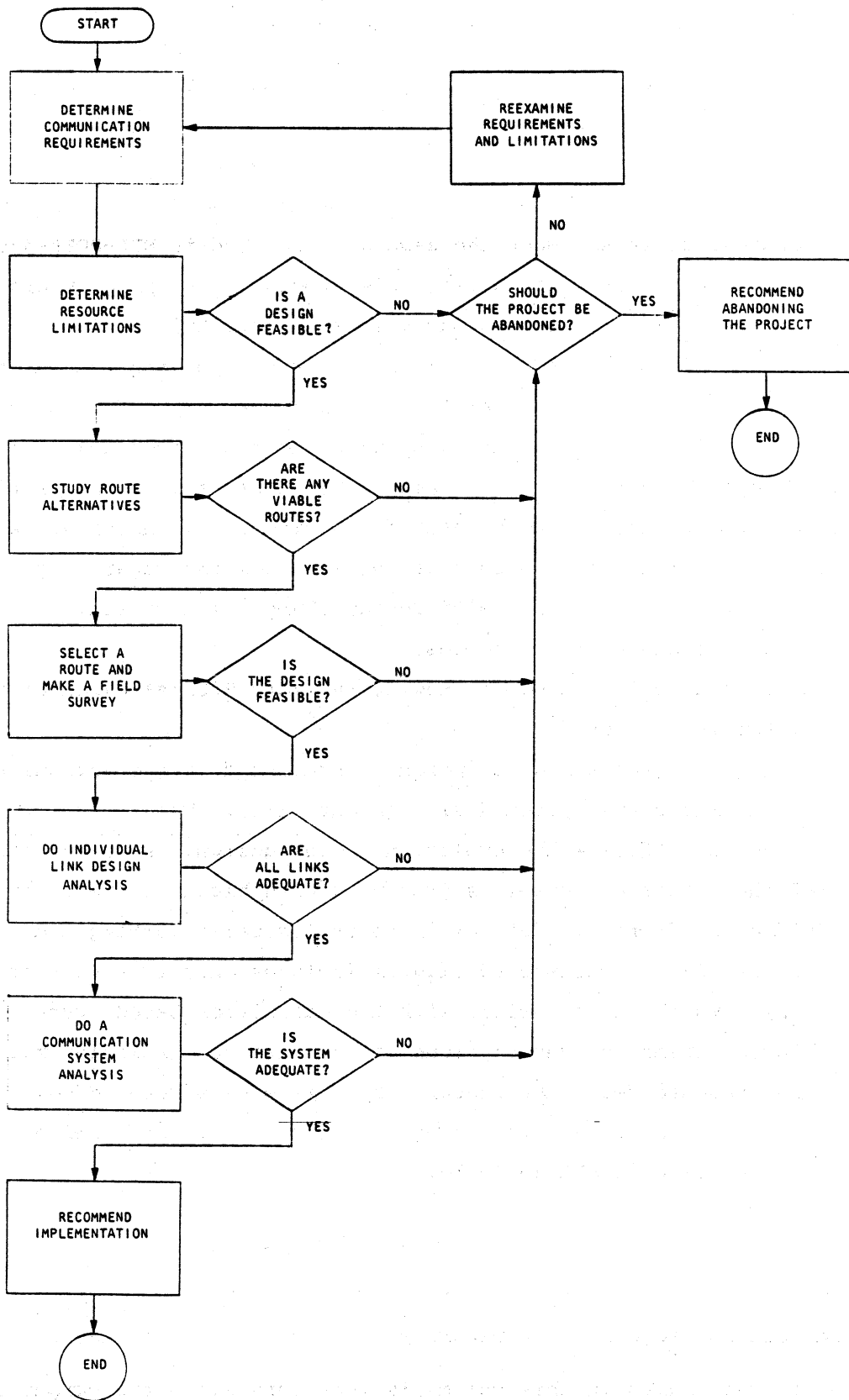


Figure 1-1. Diagram for the design of a microwave radio communication system.

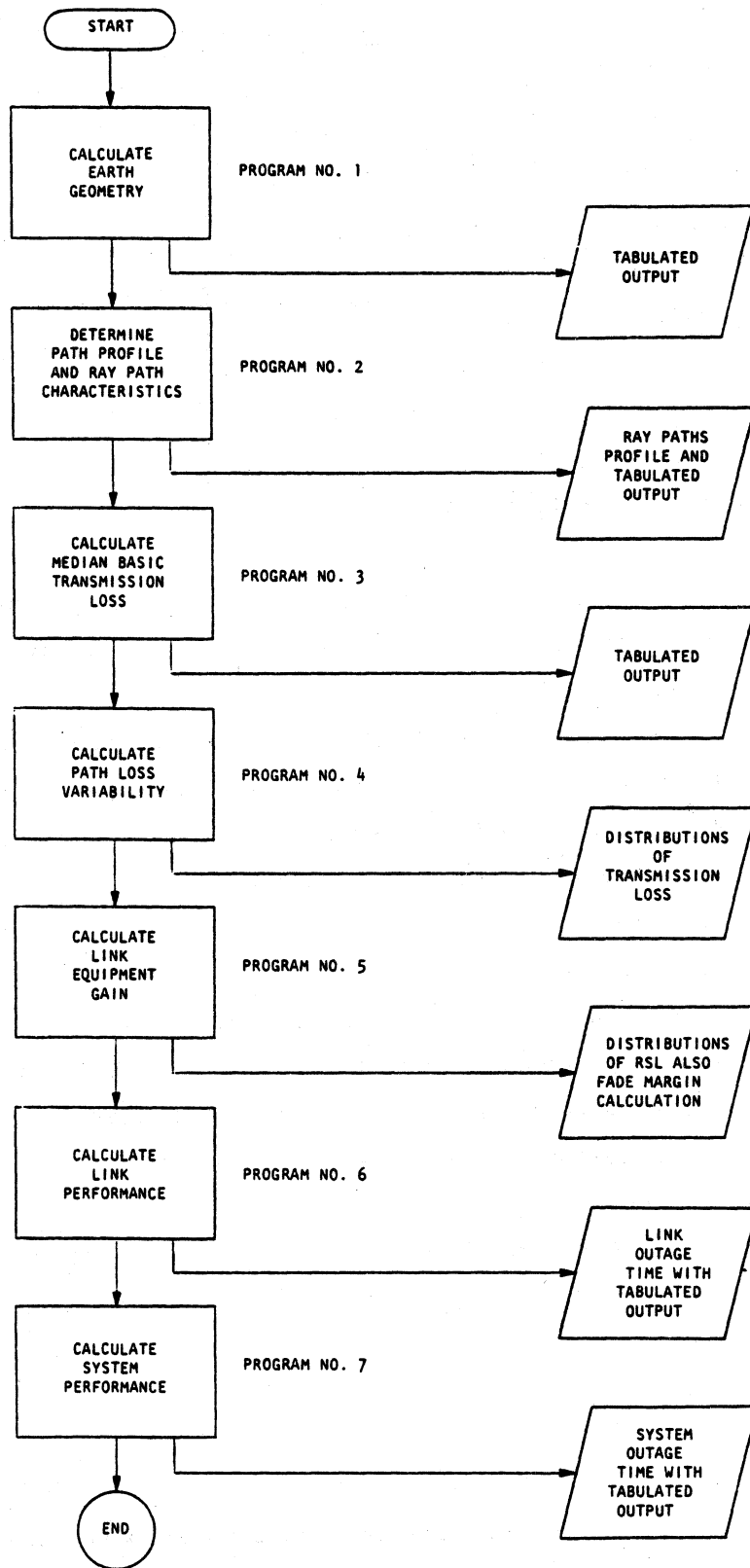


Figure 1-2. Automated system engineering model.

## Calculator Based System:

The system has five major hardware components:

1. The Calculator
2. An Impact Printer
3. An X-Y Plotter
4. A Flexible Disc Drive
5. A Hopper Card Reader

The calculator uses the HPL language (Morris et al., 1976) and has these other useful characteristics:

1. 24,000-byte working memory,
2. Built-in tape cartridge drive,
3. All of the peripheral equipment can be simultaneously connected making it possible to have the hardware always in the ready condition.

The impact printer will print the 96 ASCII (American Standard Code for Information Interchange) characters at 30 characters per second. This form of printed output was selected because it provides report-ready copy.

The X-Y plotter also provides report-ready copy. One of its features is that it can be used to digitize coordinates on the platten surface.

Some of its other major characteristics are:

1. It can draw at a rate of approximately 20 ips.
2. It is microprocessor controlled, which makes the programming of many drawing patterns and techniques practical.
3. The repeatability of pen positions is good to less than 0.01 inches.

To expand the capability of the system to handle large blocks of data, permit convenient use, and handle large numbers of complex programs, a flexible disc mass storage system was obtained. This system makes available 400,000 bytes of conveniently available memory. Each memory disc costs approximately \$10.

A hopper card reader was acquired which permits obtaining blocks of data from a large computer and entering the data into the calculator system automatically. Some examples of data which can be entered in this manner are meteorological parameters for rain-attenuation models and terrain information for plotting path profiles.

### Engineering Model Design:

The design model for a line-of-sight microwave radio communications system involves much more than making mathematical calculations and feeding in numerical values of parameters which are compared with values from standards and specifications. Figure 1-1 shows a simple diagram for the design of a microwave radio communications system. Much of the first part of the design involves making user surveys and considering lead times, funding, spectrum availability, and political realities. At the point in the evolution of the design where route alternatives are being considered, the calculator based system becomes a very useful tool for the remainder of the design process. Figure 1-2 shows a block diagram of the automated system engineering model. We will point out where the various outputs from the automated model become particularly useful in the overall design illustrated in Figure 1-1. After communications requirements and some of the resource limitations are known, calculator program Nos. 1 and 2 become useful in making preliminary studies of route alternatives from maps and other locally available sources of information. Program 2 provides information and forms vitally necessary for obtaining maximum information during the field survey. This program could be run prior to the survey. It should be rerun again after the field survey since more accurate and detailed information will then be available. If path loss measurements are going to be made during the field survey, it is also important to run programs 3 and 4 to determine expected transmission loss characteristics prior to the survey.

To select equipment properly for use on a given link, programs 2, 3, 4, 5, and 6 are necessary for rapid optimization of such things as antenna heights, antenna gains, diversity spacing, transmitter power, transmission line type, maximum transmission line return loss requirement and receiver noise figure. In the case of new systems, it is usually necessary to rerun programs 5, 6, and 7 a number of times to provide adequate system performance within reasonable cost. In the following sections, we will discuss each of the 7 basic sets of calculations and data indicated in Figure 2.

2. PROGRAM NO. 1, EARTH GEOMETRY AND PROGRAM NO. 2,  
PATH PROFILE AND RAY PATHS

The earth Geometry Program and the Path Profile and Ray Paths Program that will be discussed in this section are interdependent in that:

1. The Earth Geometry Program must be run before the Path Profile and Ray Paths Programs can be run.
2. The output tabulation from the Earth Geometry Program, except for map crossings, is included in the output tabulation of the Path Profile and Ray Paths Programs.
3. These two programs provide checks on each other by indicating differences in path length obtained by calculation from site coordinate information and path length obtained from path profile information.

The Earth Geometry Program uses the flexible disc to store data required for the execution of Program No. 2. If the data and disc are not available to Program No. 2, Program No. 2 automatically loads Program No. 1.

Program No. 1 is primarily intended as a preliminary design step for obtaining the parameters for drawing the path profile. The output of Program No. 2 is designed to provide report-ready documentation of the physical characteristics of the path profile and ray path.

A check of the great-circle path length calculated from site coordinates and the value obtained from the path profile data is desirable since path profile information and coordinates are often obtained from sources not readily accessible to the link designer. The importance of this check should not be underestimated. It has been our experience that often several sets of site coordinates are mistakenly recorded for a given site. It is the actual tower coordinates that are required. Many times named locations have more than one radio tower, several survey control points, and several surveyed structure locations. These locations lend to the confusion in specifying the proper tower coordinates.

Program No. 1 Earth Geometry:

The purpose of the Earth Geometry program is to provide a tabulation of the following data:

1. Tower (or potential tower) designations.
2. Tower base elevations above mean sea level.
3. Tower location (latitude and longitude).
4. The distance between towers.
5. Azimuth from true north at each tower to the other tower.
6. Magnetic azimuths at each tower to the other tower.
7. Map crossings (latitude and longitude).
8. Distances from map crossings to the towers.

Figure 2-1 shows a simplified block diagram for this initial program. Because the output of this program is short, it has been used as an example of program documentation and tabular output format (see Figure 2-2 and Table 2-1).

The model which we use to compute earth geometry is unavoidably inexact but should be very satisfactory for engineering line-of-sight paths. Spheroids in use today include the Clark Spheroid of 1866, the Malayan Spheroid, the Bessel Spheroid, the Australian National Spheroid, and the International Spheroid. Table 2-2 lists the equatorial and polar radii in kilometers and an arithmetic average of these. Conversion factors between degrees and distance on the surface of a sphere of radius equal to either the equatorial or polar radius are included, as well as an arithmetic average of the factors for each spheroid. These conversion factors are only valid exactly at the pole or on the equator, but the American Ephemeris and Nautical Almanac for the year 1975 (1973) page 528, gives equations for approximating the true arc length of the International Spheroid.

$$1^\circ \text{ latitude} = 111133.35 - 599.84 \cos 2\phi + 1.17 \cos 4\phi \text{ meters, and} \quad (2-1)$$

$$1^\circ \text{ longitude} = 111413.28 \cos \phi - 93.51 \cos 3\phi + 0.12 \cos 5\phi \text{ meters} \quad (2-2)$$

where  $\phi$  is the mid-latitude of the arc.

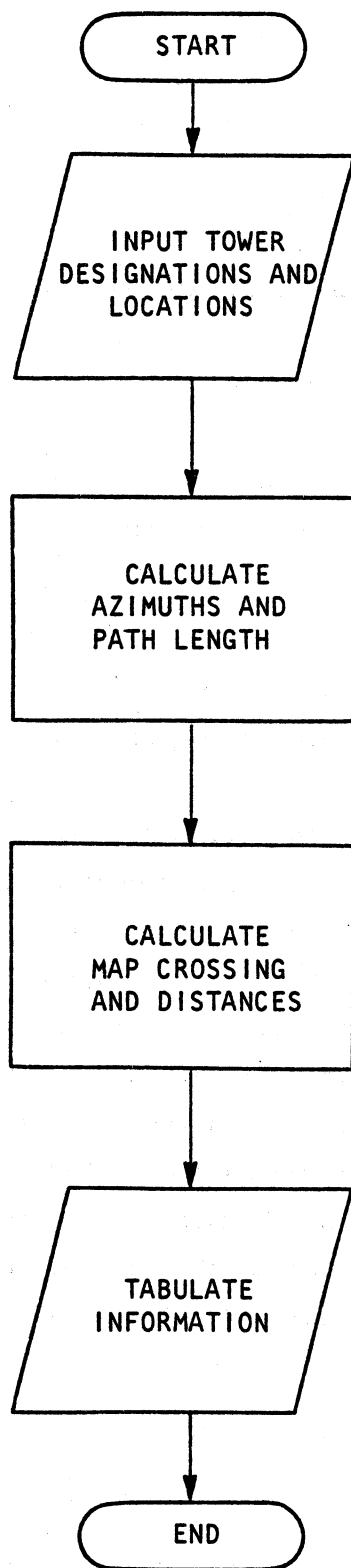


Figure 2-1. Earth geometry model.

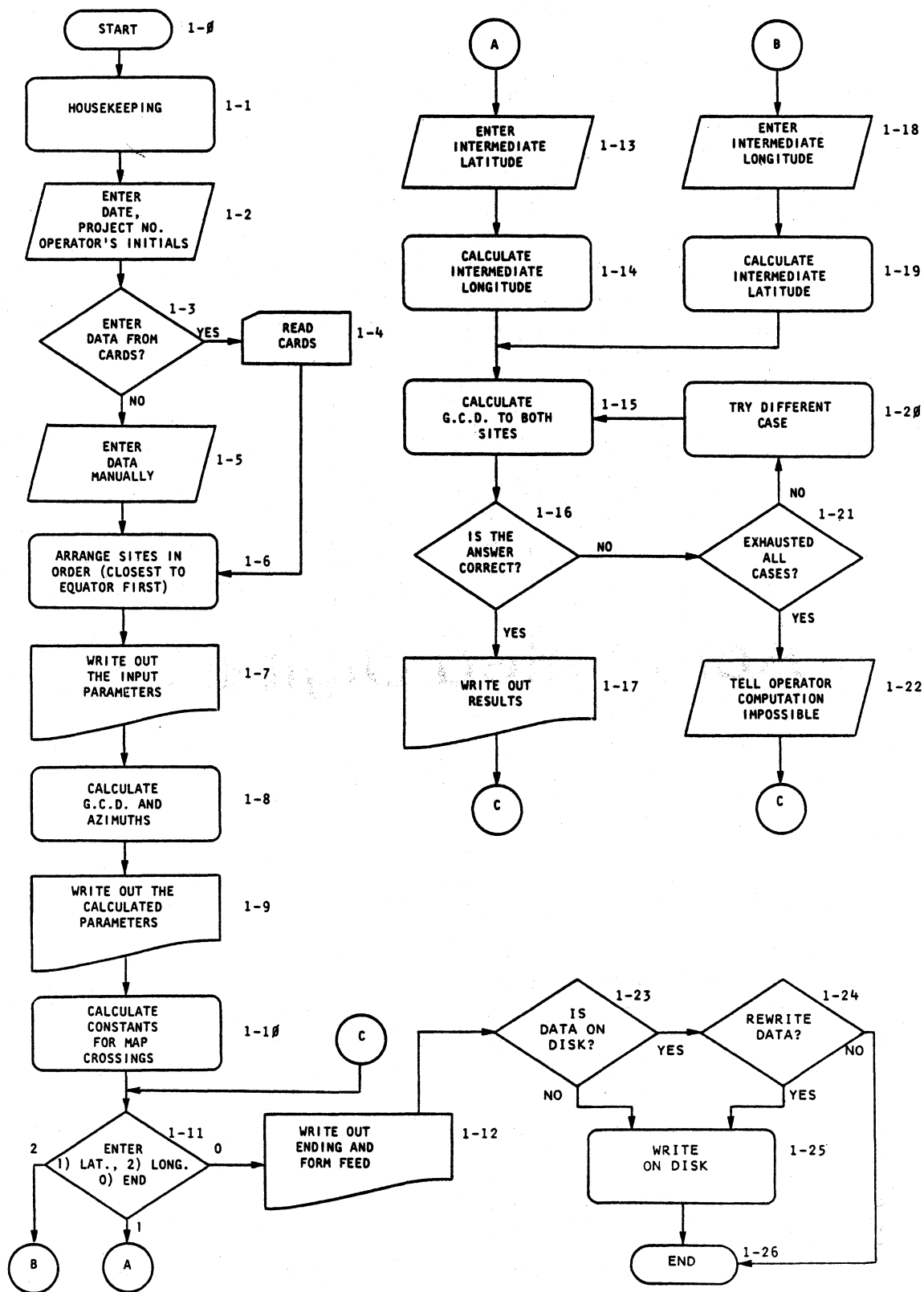


Figure 2-2. Earth geometry program flow chart.

Table 2-1. Example of an Earth Geometry Tabular Output

Earth Geometry for the LANGERKOPF-FELDBERG Path

31 Jan 78 - Project No: 789456123 - DRW  
(MKS units)

Tower Name	Designator	Latitude deg min sec	Longitude deg min sec	Elev (MSL) meters
LANGERKOPF	LKF 1	49 18 04.0N	7 50 47.0E	602.0
FELDBERG	FEL 0	50 14 33.0N	8 29 49.0E	688.8

-----  
Great circle distance between towers is 114.55 kilometers

Azimuths from TRUE NORTH: deg min sec  
Azimuth from LKF to FEL is 23 48 13.55  
Azimuth from FEL to LKF is 204 18 01.69

Declination of MAGNETIC NORTH from TRUE NORTH:  
deg min  
At LANGERKOPF 12 07.0W  
At FELDBERG 12 03.0W

Azimuths from MAGNETIC NORTH: deg min  
Azimuth from LKF to FEL is 11 41.2  
Azimuth from FEL to LKF is 192 15.0

-----  
Intermediate coordinates (Map crossings):

Latitude deg min sec	Longitude deg min sec	Distance (km) from:	
		LKF	FEL
49 30 00.00N	7 58 53.53E	24.16	90.39
50 00 00.00N	8 19 36.08E	85.00	29.55
49 31 37.33N	8 00 00.00E	27.45	87.10

-----  
(Program Version: 24Jan78)

Table 2-2. Earth Radius For Various Spheroids

Spheroid	Equatorial Radius	Polar Radius	Average Radius	Conversion Equatorial/Polar		Average
International	6378.388	6356.912	6367.65	111.3239	110.9490	111.1365
Clark 1866	6378.2064	6356.5838	6367.3951	111.3207	110.9433	111.1320
Clark 1880	6378.249145	6356.514869	6367.382005	111.3214	110.9421	111.1318
Everest	6377.276345	6356.075415	6366.67588	111.3045	110.9344	111.1195
Bessel	6377.397155	6356.078963	6366.73806	111.3066	110.9345	111.1205
Australian National	6378.160	6356.7745	6367.46735	111.3199	110.9466	111.1333
Airy	6377.563396	6356.256910	6366.910155	111.3095	110.9376	111.1235
Fischer	6378.155	6356.77332	6367.46416	111.3198	110.9466	111.1332
Malayan	6377.304063	6356.103039	6366.70355	111.3050	110.9349	111.1199

At a recent meeting of the International Astronomical Union, the system of Astronomical Constants was revised to reflect the adoption of the values of the Australian National Spheroid as the current standard in the System of Astronomical Constants. Although there are differences in the several spheroids in present use, these differences are still not resolved, nor perhaps resolvable since satellite measurements indicate that the Earth is not a true spheroid. For a further discussion of the determination of the various spheroids see for example "Dynamic Geodesy" by Kamela (1964). A map showing which areas of the world are based on the various spheroids is contained in U.S. Army TM 5-241-1 (1967). Thus, for greatest accuracy, the applicable spheroid constants can be used in any particular area of the world.

However, lest we lose sight of the relative importance of the accuracy and precision required of the spheroid constants, it should be pointed out that the distance factor derived from the equatorial and polar Earth radii is used in LOS system calculations primarily to determine transmission loss in free space. The distance term in this equation is  $20 \log d$  and the error introduced into the transmission loss value by using the widest spread of values from Table 2-2 is bounded by

$$20 \log \frac{111.3239}{110.9344}$$

which is of the order of 0.03 dB.

The information used to compute azimuth from true north and path length is essentially the same as that in MIL-HDBK-416 (1977) pp. 4-36 thru 4-39. The spherical triangle on a unit radius sphere used for the computation of points on a great circle path is identified on Figure 2-2 as PAB. Points A and B are the antenna terminals, and P is the north or south pole. Point B is selected to have a greater latitude than A. The triangle shown is for the northern hemisphere but may readily be inverted to apply to the southern hemisphere. The latitudes of the points are denoted by  $L_A$  and  $L_B$ , while C is the difference in longitude between A and B. Angle Z multiplied by the Earth's radius is the corresponding great-circle path length. The following formulas are practical for hand computations as well as for digital computers. Equations 2-3 to 2-7 have been taken from ITT (1975) (pp. 28-9 to 28-11).

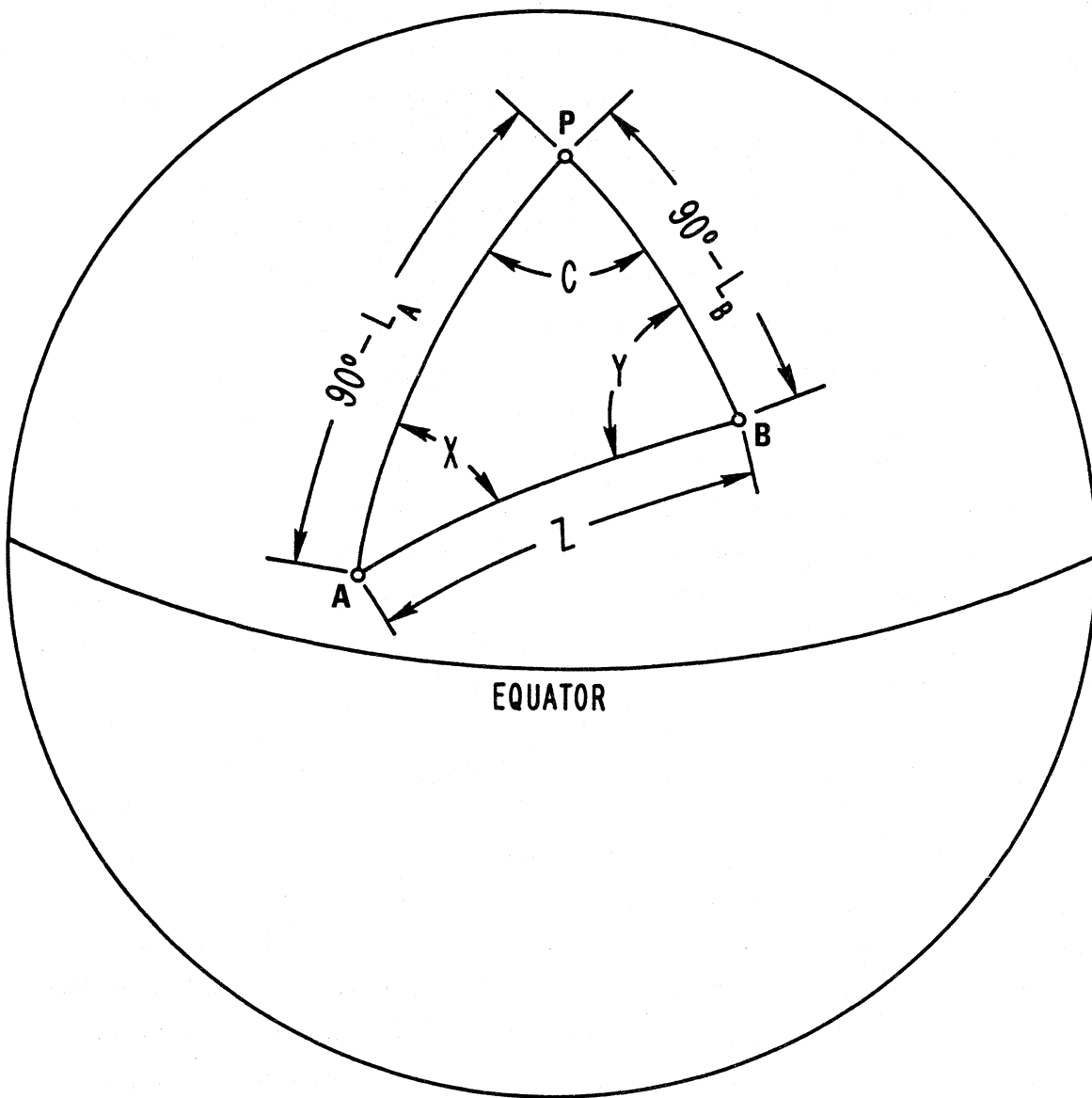


Figure 2-3. Spherical triangle for great-circle path computations.

The initial bearings or azimuth values (X from terminal A, and Y from terminal B) are measured from true north, and are calculated as follows:

$$\tan \frac{Y - X}{2} = \left( \cot \frac{C}{2} \right) \left( \sin \frac{L_B - L_A}{2} \right) / \left( \cos \frac{L_B + L_A}{2} \right) \quad (2-3)$$

$$\tan \frac{Y + X}{2} = \left( \cot \frac{C}{2} \right) \left( \cos \frac{L_B - L_A}{2} \right) / \left( \sin \frac{L_B + L_A}{2} \right) \quad (2-4)$$

$$\frac{Y + X}{2} + \frac{Y - X}{2} = Y, \text{ and } \frac{Y + X}{2} - \frac{Y - X}{2} = X. \quad (2-5)$$

The great-circle distance, Z (in degrees), is given by

$$\tan \frac{Z}{2} = \left( \tan \frac{L_B - L_A}{2} \right) \left( \sin \frac{Y + X}{2} \right) / \left( \sin \frac{Y - X}{2} \right). \quad (2-6)$$

To convert the angle Z obtained in degrees to kilometers, the following is used:

$$D_{\text{km}} = 111.12 Z^\circ. \quad (2-7)$$

The following formulas show how to calculate either the latitude or the longitude of a point on the great-circle path, when the other coordinate is given. The given coordinates often correspond to the edges of detailed maps, and to intermediate points usually about 7.5 minutes apart, so that straight lines between points will adequately approximate a great-circle path.

The basic map crossing equations may be derived by calculating the intersection of the equation of a sphere and the equation of a plane through the origin at the center of the sphere in terms of latitudinal and longitudinal coordinates. The symbol for latitude is L and for longitude  $\lambda$ . The angle values for north latitude are considered positive and for south latitude they are negative. The angle values for east longitude are positive and for west longitude they are negative. The equation for this intersection (all great-circle paths) is:

$$\tan L = k_1 \sin \lambda + k_2 \cos \lambda \quad (2-8)$$

where  $k_1$  and  $k_2$  are constants for any particular great-circle path. Another form of this equation is:

$$\tan L = k_3 \sin (\lambda + k_4) \quad (2-9)$$

where  $k_3$  and  $k_4$  are also constants for any particular great-circle path.

The relationship between the two sets of constants are:

$$k_3 = \frac{k_2}{\sin k_4} \quad \text{or} \quad k_3 = \frac{k_1}{\cos k_4} \quad (2-10)$$

and

$$k_4 = \tan^{-1} (k_2/k_1). \quad (2-11)$$

Since the tower coordinates for A and B are usually known, these coordinate values ( $L_A, \lambda_A$ ) and ( $L_B, \lambda_B$ ) may be used to calculate the great-circle path constants:

$$k_4 = \tan^{-1} \left[ \frac{\tan L_B \sin \lambda_A - \tan L_A \sin \lambda_B}{\tan L_A \cos \lambda_B - \tan L_B \cos \lambda_A} \right] \quad (2-12)$$

$$k_3 = \frac{\tan L_A}{\sin (\lambda_A + k_4)} \quad \text{or} \quad k_3 = \frac{\tan L_B}{\sin (\lambda_B + k_4)}. \quad (2-13)$$

With values for these constants, the intersection of the great-circle path with any value of latitude or longitude may now be calculated provided that it exists (some great-circle paths do not intersect some latitudes). The explicit expressions for latitude in terms of longitude and longitude in terms of latitude are:

$$L = \tan^{-1} \left[ k_3 \sin (\lambda + k_4) \right] \quad (2-14)$$

and

$$\lambda = \sin^{-1} \left( \frac{\tan L}{k_3} \right) - k_4. \quad (2-15)$$

Program No. 2, Path Profile and Ray Path Characteristics:

The purpose of this program is to help provide the designer with an accurate set of information about the radio path. The goals are optimum selection of antenna heights and the preparation of foundation information to estimate the radio path reliability.

Figure 2-4 is a diagram of the terrain profile and ray-path model. The ray paths are calculated in accordance with the procedures in MIL-HDBK-416 (1977).

Initially, the program should be used to help with the process of route selection. After a route has been selected, the program can be used to supply forms and information for the field survey. Often preliminary information is not accurate and such forms prompt the field survey engineer to obtain both accurate and complete information. For example, coordinates for one of the towers obtained early in the design process may turn out to have been coordinates for an older tower. Such discrepancies often become apparent on the site survey and a complete set of forms prompts a thorough search for the required information especially if the information input to the calculator is printed out in the same format as that required for filling out the site survey forms. After the field survey has been completed, this program should be rerun using the new information to insure an accurate foundation for link outage time predictions.

The output of this program is in two parts; one part is a path profile with ray paths drawn for a diversity configuration (normally on 11 x 17 inch paper) and the second part is a tabular summation of meteorological, geographical and other required information about the path (see Figure 2-5 and Table 2-3). Some information common to the output from Program 1 is presented again on the tabulation (coordinates, heights, etc.).

Several simple models are used to find parameters that are used in various steps of the system design. These models are needed to calculate ray path geometry, Fresnel-zone clearance, minimum path clearance above obstacles and terrain, ray take-off angle at the antenna, minimum atmospheric layer penetration angle,\* mean atmospheric pressure along the ray path and mean height of the ray path above ground.

---

\*The term penetration angle as used here means penetration angle of atmospheric layers concentric with the center of the earth.

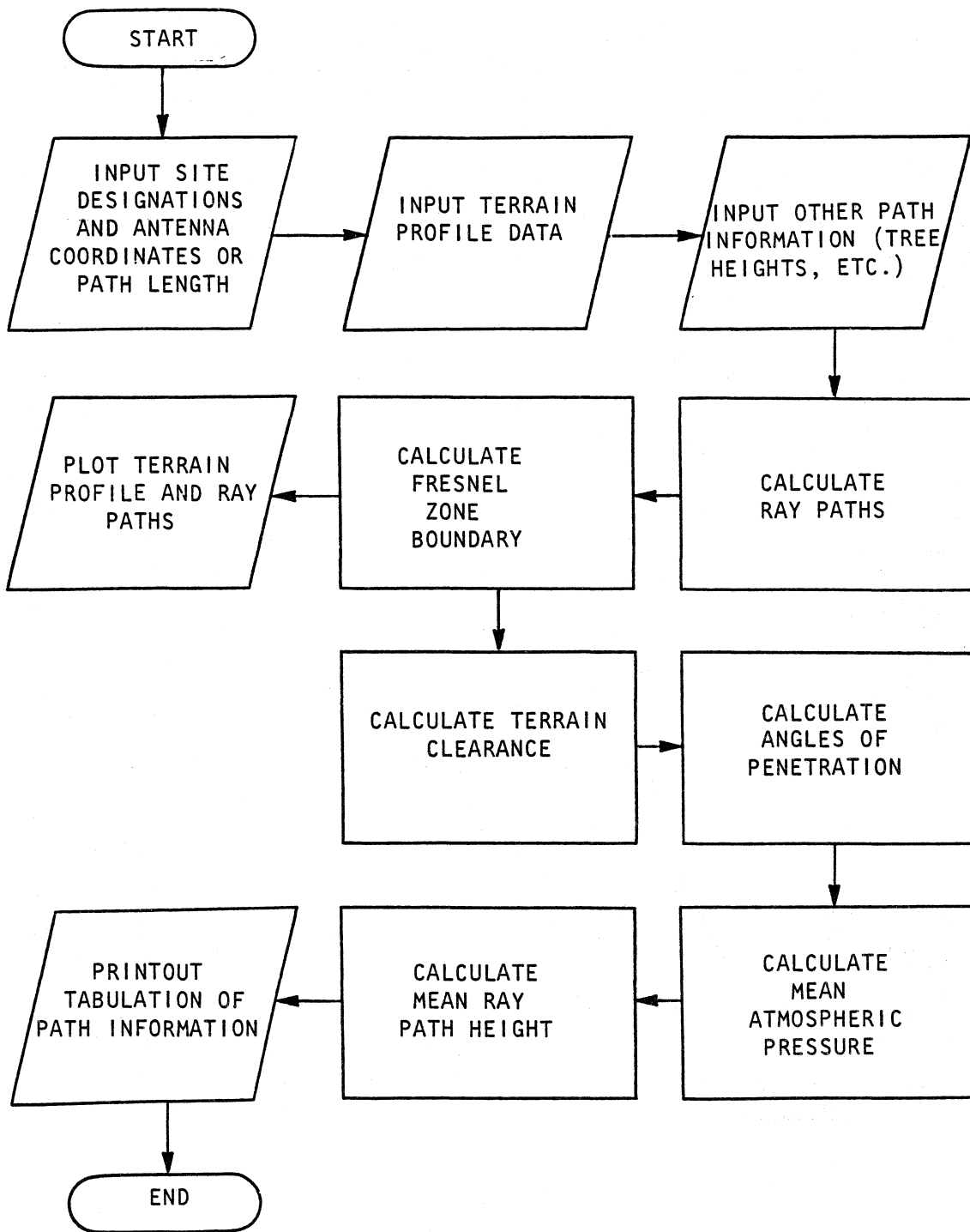


Figure 2-4. Terrain profile and ray-path model.

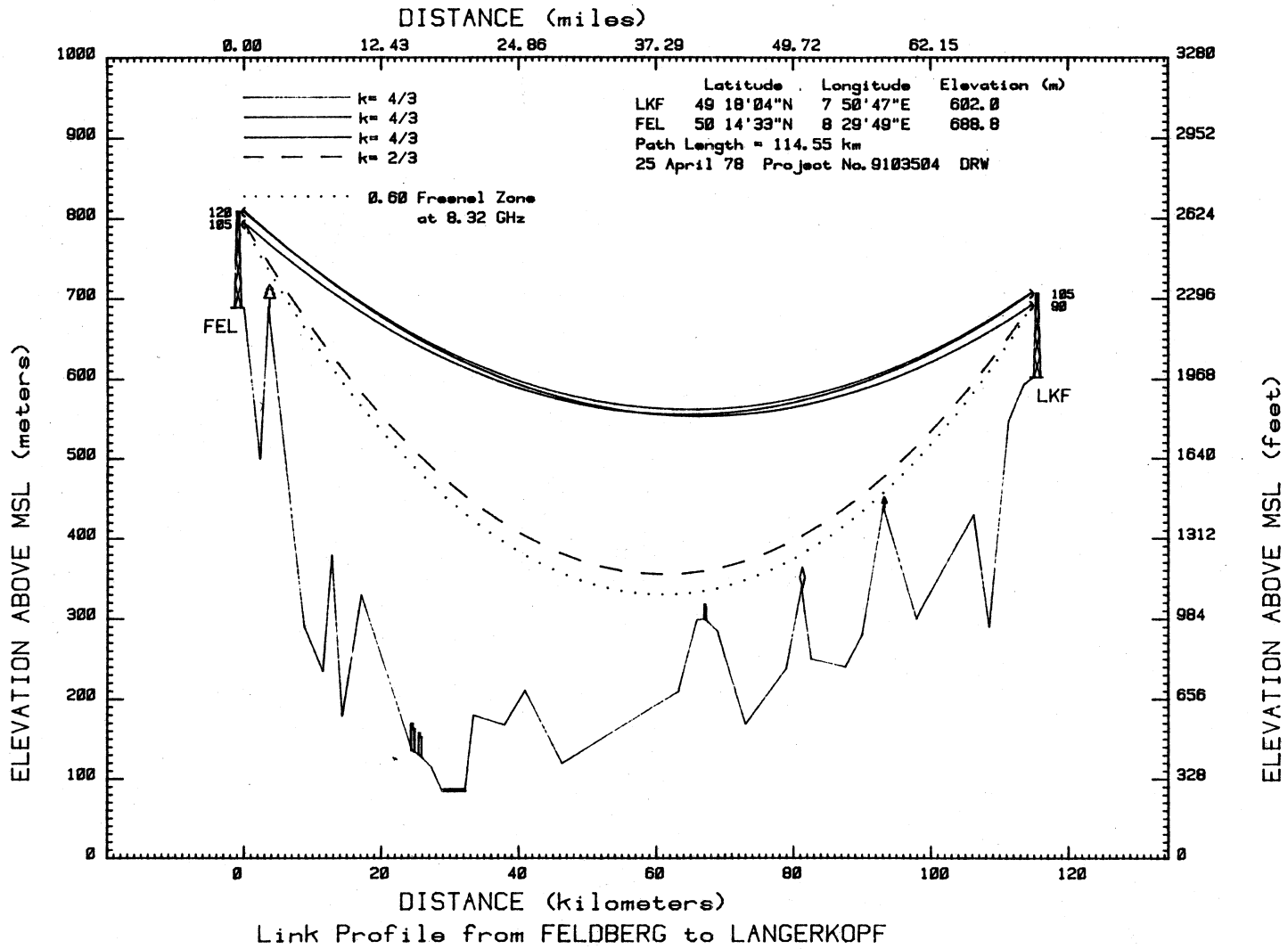


Figure 2-5. Example of terrain profile and ray paths.

Table 2-3. Example of Microwave Path Tabulation

Terrain Profile and Ray Path Information  
for the FELDBERG, LANGERKOPF Link  
27Jul78 Project No. 9103504 THH

COORDINATES:

Site	Latitude	Longitude	Elevation above MSL	Heights Above Ground	
				Upper Ant	Lower Ant
FEL 0:	50 14'33"N	8 29'49"E	688.8m	120.0m	103.0m
LKF 1:	49 18'04"N	7 50'47"E	602.0m	105.0m	90.0m

PATH LENGTH:

Path Length is 114.55 kilometers

PATH AZIMUTHS:

Azimuths from True North:

LKF 1 to FEL 0 23 48'14"  
FEL 0 to LKF 1 204 18'02"

Azimuths from Magnetic North:

LKF 1 to FEL 0 11 41'14"  
FEL 0 to LKF 1 192 15'02"

RAY PATH MINIMUM CLEARANCE:

For an Earth Radius Factor of  $k=0.67$ :

Absolute clearance is 24.37 meters at 93.18 km from FEL.  
Minimum clearance is 0.94 Fresnel Zones at 8.20 GHz,  
and 93.18 km from FEL.

Table 2-3. Example of Microwave Path Tabulation  
(Sheet 2)

Terrain Profile and Ray Path Information (continued)  
for the FELDBERG, LANGERKOPF Link

ANGLES OF ATMOSPHERIC PENETRATION:

For an Earth Radius Factor of  $k= 1.33$ :  
Take off angle at LKF 1 is  $-0.44$  degrees.  
Take off angle at FEL 0 is  $-0.34$  degrees.  
Minimum angle of penetration is  $0.00$  degrees.

PATH NOTES:

1. Mean atmospheric pressure on the path is  $p_m = 93.96$  kPa
2. Mean Path height for  $k=4/3$  is  $h_m = 321.20$  meters.
3. Has an allowance for growth been included in the tree heights shown on the profile?
4. The terrain is typical of Mountains.
5. The estimated annual worst month average snow depth at the location of minimum clearance is  $3.00$  m.
6. Additional comments: (entered by operator)  
New construction is planned near LKF site.

Table 2-3. Example of Microwave Path Tabulation  
(Sheet 3)

Profile Data for the Path from  
FELDBERG Tower 0 to LANGERKOPF Tower 1  
25 April 78 Project No. 9103504 DRW

Point No.	Metric Units			English Units		
	Dist (km)	Elev (m)	Code Height (m)	Dist (mi)	Elev (ft)	Code Height (ft)
1	0.00	689		0.00	2261	0
2	2.35	500		1.46	1641	0
3	3.56	690	Tree	2.21	2264	Tree 92
4	8.85	290		5.50	951	0
5	11.53	235		7.16	771	0
6	12.85	380		7.98	1247	0
7	14.35	179		8.92	587	0
8	17.15	330		10.66	1083	0
9	24.55	136	Bldg	15.25	446	Bldg 112
10	24.65	136	Bldg	15.32	446	Bldg 112
11	24.85	135		15.44	443	0
12	25.67	130	Bldg	15.95	427	Bldg 92
13	27.35	115		16.99	377	0
14	28.92	85	Water	17.97	279	Water 0
15	32.20	85	Water	20.01	279	Water 0
16	33.43	180		20.77	591	0
17	37.95	168		23.58	551	0
18	40.95	211		25.45	692	0
19	46.34	120		28.79	394	0
20	63.25	210		39.30	689	0
21	65.95	299		40.98	981	0
22	67.15	300	Bldg	41.72	984	Bldg 59
23	68.97	285		42.86	935	0
24	73.05	169		45.39	554	0
25	79.00	238		49.09	781	0
26	81.23	339	Obst	50.47	1112	Obst 82
27	82.67	250		51.37	820	0
28	87.65	240		54.46	787	0
29	90.10	280		55.99	919	0
30	93.18	440	Tree	57.90	1444	Tree 39
31	98.00	300		60.89	984	0
32	98.50	310		61.20	1017	0
33	106.29	430		66.05	1411	0
34	108.54	290		67.44	951	0
35	111.35	547		69.19	1795	0
36	113.55	593		70.56	1946	0
37	114.85	602		71.36	1975	0

The geometry of the ray path is considered in section 4.2.15 of MIL-HDBK-416 (1977) and the expression for the height of the ray path,  $h$ , in meters above mean sea level (m.s.l.) is as follows:

$$h = \frac{1}{12.75k} d^2 + \left\{ \frac{h_2 - h_1}{D} - \frac{D}{12.75k} \right\} d + h_1 \quad (2-16)$$

where  $h_1$  = the antenna height in meters above m.s.l. where  $d = 0$ .

$h_2$  = the antenna height in meters above m.s.l. where  $d = D$ .

$d$  = the distance along the path in km.

$D$  = the length of the path in km.

$k$  = the Earth's radius factor.

In MIL-HDBK-416, (1977) section 4.2.18 an equation is provided for calculating the  $n$ th Fresnel-zone radius,  $R_n$ , on a plane perpendicular to the path:

$$R_n = 17.3 \frac{(n)^{1/2}}{f} \left( \frac{dD - d^2}{D} \right)^{1/2} \text{ m}, \quad (2-17)$$

where  $f$  = frequency in GHz.

The clearance,  $C$ , is the distance between the top of the obstacle directly beneath the ray path and the ray path in meters.

The number of Fresnel zones,  $n$ , is given by the following expression:

$$n = \frac{3.34 fDC^2}{dD - d^2} \times 10^{-3}. \quad (2-18)$$

For all entered values of  $d$  along the path,  $n$  is calculated and the minimum value of  $n$  with the corresponding value of  $d$  is recorded.

The take-off angle,  $\beta$ , is the angle between the horizontal plane and the tangent to the ray path at an antenna.

When  $d = 0$ ,

$$\beta_1 = \tan^{-1} \left( \frac{h_2 - h_1}{1000 \times D} - \frac{D}{12750k} \right). \quad (2-19)$$

When  $d = D$ ,

$$\beta_2 = -\tan^{-1} \left( \frac{D}{12750k} + \frac{h_2 - h_1}{1000 \times D} \right). \quad (2-20)$$

If  $\beta_1 < 0$  and  $\beta_2 < 0$ , then the minimum angle of penetration is 0.

If  $|\beta_1| < |\beta_2|$ , the minimum angle of penetration is  $|\beta_1|$  for  $k > 0$ .

If  $|\beta_1| > |\beta_2|$ , the minimum angle of penetration is  $|\beta_2|$  for  $k > 0$ .

To calculate the mean atmospheric pressure along the path, we will use the expression for pressure,  $p$ , as a function of altitude,  $h$ , in meters above mean sea level provided in List (1951), pp. 266.

$$p = 101.3 (1 - 2.26h \times 10^{-5})^{5.2553} \quad (-100 < h < 10^5) \quad (2-21)$$

where  $p$  is the atmospheric pressure in kilopascals (kPa), the mean pressure  $\bar{p}$  can be calculated by averaging the 10 values of  $p$  calculated for 10 equidistant points along the path calculated for  $k = 4/3$ .

To estimate the average height above ground,  $\Delta h$ , we calculate the difference between  $h$  and the terrain height above mean sea level,  $h_t$ , at 10 approximately equidistant points along the path and calculate the arithmetic average,  $\overline{\Delta h}$ , in meters.

### 3. PROGRAM NO. 3, MEDIAN BASIC TRANSMISSION LOSS MODEL

The model for calculating median basic transmission loss is similar to the model in MIL-HDBK-416 (1977). It is based on the inverse square law and the gas absorption model (Figure 3-1). Terrain reflections are not a part of this model although for low antennas and particularly smooth terrain, reflections can strongly influence the median received signal level. Over the frequency range of interest here (1 to 50 GHz), the adverse effects of terrain reflections on signal level are usually overcome by using space diversity. For this reason, we are not including terrain reflection effects in the median basic transmission loss calculation. We do not want to imply that terrain reflection effects should be ignored in the design of a system. Aside from affecting received signal level, reflections may cause a delayed signal distortion of the desired signal, therefore they should be avoided if possible. Another factor which will affect median basic transmission loss is partial blocking of the ray path by an obstacle. Such an obstacle produces a diffracted field. Basic transmission loss may be estimated for the diffraction path using the diffraction theory included in MIL-HDBK-416 (1977) but these estimates are not included in the calculator model.

The basic free-space transmission loss,  $L_{bf}$ , is calculated as follows:

$$L_{bf} = 92.45 + 20 \log f_{\text{GHz}} + 20 \log d_{\text{km}} \quad \text{dB} \quad (3-1)$$

where  $d_{\text{km}}$  is distance in km and  $f$  is frequency in GHz.

The atmospheric absorption loss component due to oxygen is dependent primarily on air density and path length and is fairly stable as a function of time. The component due to water vapor absorption, on the other hand, varies with air density, temperature, and humidity which requires a more complicated model to predict a median value. The first water vapor line occurs at 22 GHz with substantial effects at frequencies above 15 GHz. The graph often used to estimate water vapor absorption assumes a value of absolute humidity of about  $10 \text{ g/m}^3$  (MIL-HDBK-416, 1977, p. 4-49). In many parts of the world absolute humidity will remain between 20 and  $30 \text{ g/m}^3$  for weeks at a time, therefore a better model than the one used in MIL-HDBK-416 (1977) is required. The model which we use for calculating atmospheric absorption is one prepared by H.J. Liebe and G.G. Gimmestad (1978). Atmospheric absorption,  $A_{\alpha}$ , is calculated by adding the components due to oxygen and water vapor:

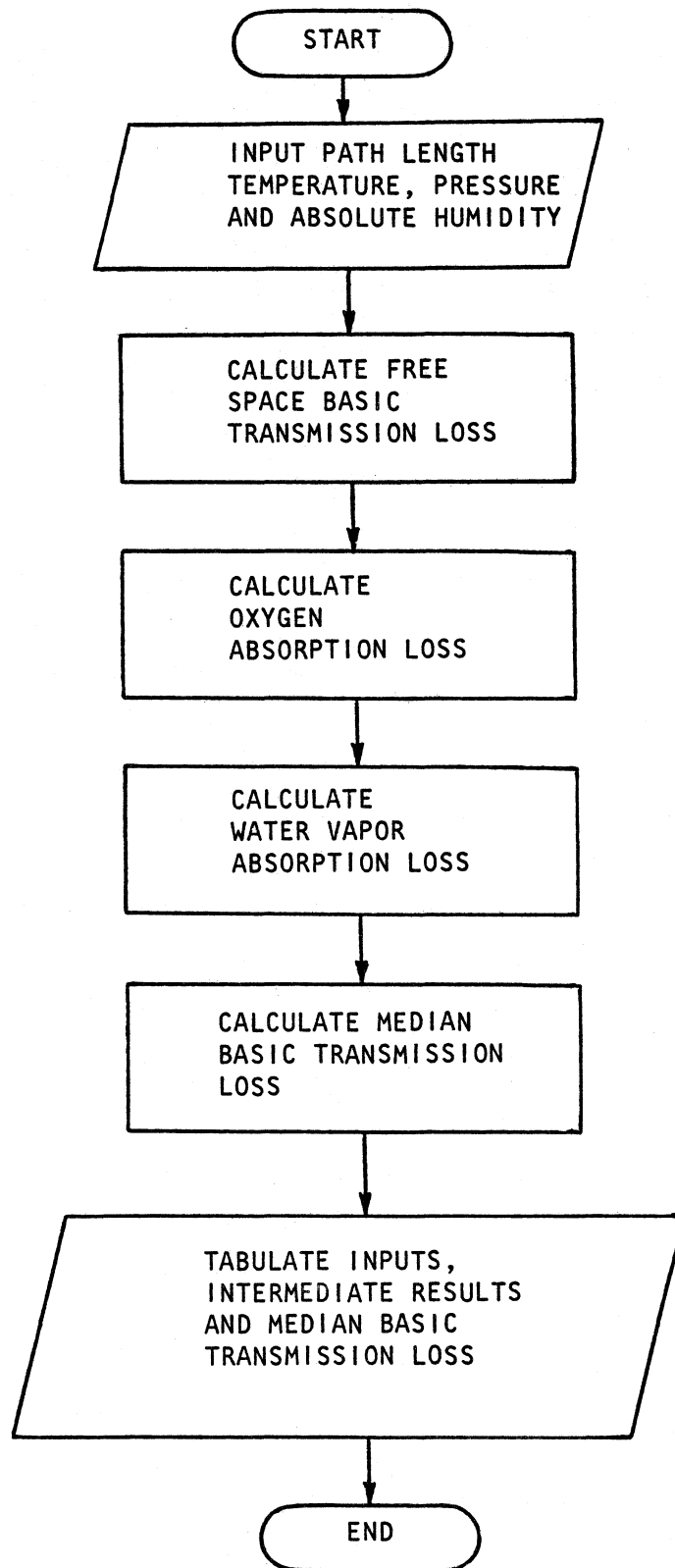


Figure 3-1. Median basic transmission loss model.

$$A_{\alpha} \sim d_{\text{km}} (\alpha_1 + \alpha_2). \quad (3-2)$$

To calculate  $O_2$  absorption per unit length,  $\alpha_1$ , to 50 GHz:

$$\alpha_1 = \frac{0.626 \times 10^{-6} f^2 p^2 t^{2.9}}{f^2 + 3.14 \times 10^{-5} p^2 t^{1.8}} + 0.1820 f \sum_{a=1}^{a=36} S_a F_a'' \quad (3-3)$$

$$S_a = A_1 p t^3 \exp [A_2 (1-t)] \quad (3-4)$$

$$F_a'' = \frac{f}{f_a} \left( \frac{\gamma_a - (f_a - f) I_a}{(f_a - f)^2 + \gamma_a^2} + \frac{\gamma_a - (f_a + f) I_a}{(f_a + f)^2 + \gamma_a^2} \right) \quad (3-5)$$

$$\gamma_a = A_3 (p + 1.3 p_w) t^{0.9} \quad (3-6)$$

$$I_a = A_4 p t^2 \quad (3-7)$$

$f$  = frequency in GHz. ( $1 < f < 50$ )

$f_a$  = line frequency (see Table 3-1)

$$t = \frac{300}{T+273.16} \quad \text{where } T = \text{temperature in } ^\circ\text{C}. \quad (3-8)$$

( $-98 < T < 37$ )

$T$  is the median path air temperature.

For the value of  $T$ , a world map of mean temperature values is provided (Fig. 3-2). A default value\* is  $T = 20^\circ\text{C}$ .

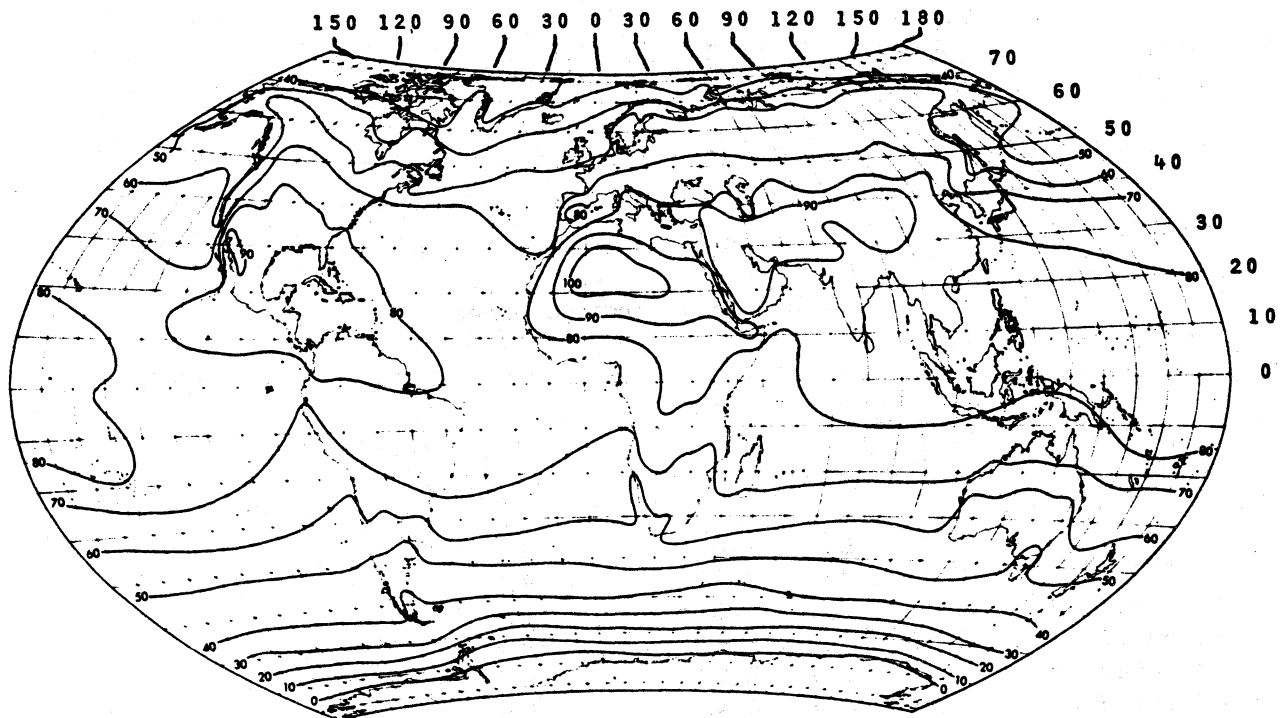
$$p = p_m - p_w \quad (60 < p_m < 101.3). \quad (3-9)$$

$p_m$  is the mean air pressure on the radio path.

It is provided as an output of the path profile and ray path program. A default value\* is  $p_m = 101.3$  kPa (pressure at mean sea level).

\*The term default value as used here means a value for making an estimate when a more accurate value is not available.

**AVERAGE JULY TEMPERATURE (F°)**



Degrees Celsius =  $\frac{5}{9} (\text{°F}-32)$

**AVERAGE JANUARY TEMPERATURE (F°)**

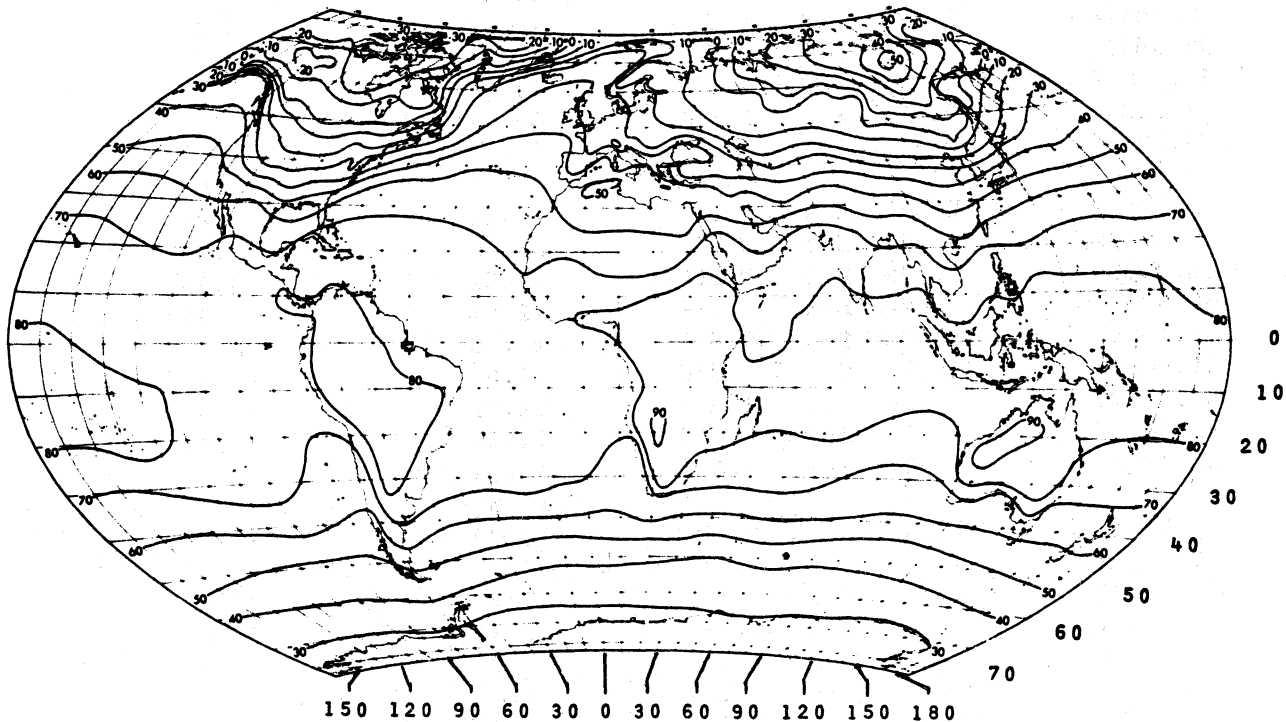


Figure 3-2. Mean temperature values (use July values for the Northern Hemisphere and January values for the Southern Hemisphere). (From "Climates of the World", U.S. Dept. of Comm., ESSA, Environmental Data Service, January 1969.)

$$p_w = 0.00046151 \rho_w (T + 273.16) \quad (3-10)$$

$\rho_w$  = air water vapor density in  $g/m^3$ . ( $0 < \rho_w < 40$ )

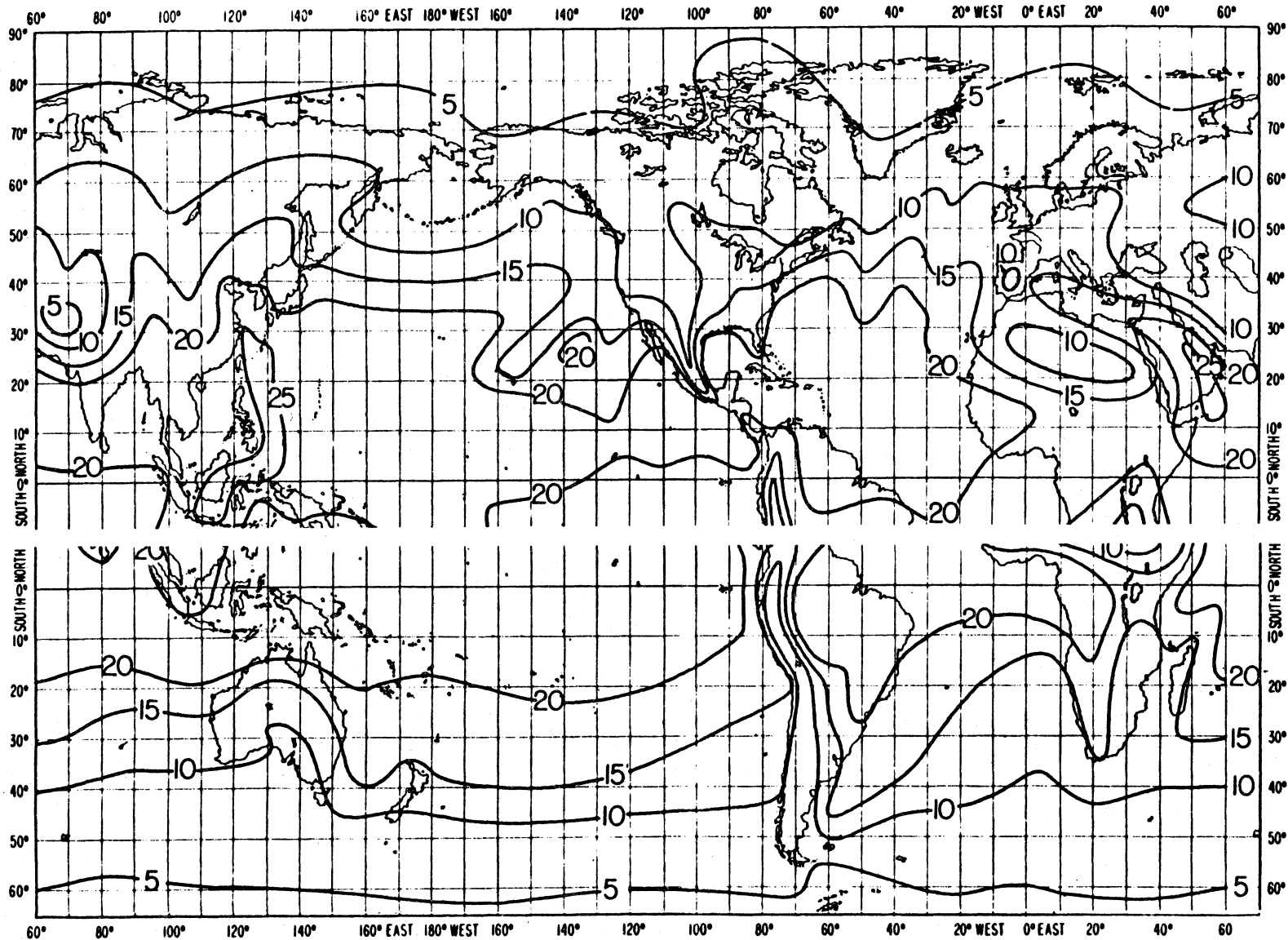
For the value of  $\rho_w$ , a world contour map is provided (Fig.

3-3). A default value for water vapor density is  $\rho_w = 15 g/m^3$ .

For values of  $f_a$ ,  $A_1$ ,  $A_2$ ,  $A_3$  and  $A_4$ , see Table 3-1.

Table 3-1. Oxygen Lines

Center Frequency $f_a$ (GHz)	Strength		Width $A_3$ ( $\frac{GHz}{kPa}$ )	Interference $A_4$ ( $\frac{1}{kPa}$ )
	$A_1$ ( $\frac{kHz}{kPa}$ )	$A_2$		
50.9873	2.44	E-6 8.69	$8.7 \times 10^{-3}$	$5.5 \times 10^{-3}$
51.50302	6.04	E-6 7.74	8.9 "	5.6 "
52.02117	1.41	E-5 6.84	9.2 "	5.5 "
52.54223	3.08	E-5 6.00	9.4 "	5.7 "
53.06680	6.37	E-5 5.22	9.7 "	5.3 "
53.59572	1.24	E-4 4.48	10.0 "	5.4 "
54.12997	2.265	E-4 3.81	10.2 "	4.8 "
54.67116	3.893	E-4 3.19	10.5 "	4.8 "
55.22136	6.274	E-4 2.62	10.79 "	4.17 "
55.78380	9.471	E-4 2.11	11.10 "	3.75 "
56.26478	5.453	E-4 0.0138	16.46 "	7.74 "
56.36339	1.335	E-3 1.66	11.44 "	2.97 "
56.96818	1.752	E-3 1.255	11.81 "	2.12 "
57.61249	2.126	E-3 0.910	12.21 "	0.94 "
58.32389	2.369	E-3 0.621	12.66 "	-0.55 "
58.44660	1.447	E-3 0.0827	14.49 "	5.97 "
59.16422	2.387	E-3 0.386	13.19 "	-2.44 "
59.59098	2.097	E-3 0.207	13.60 "	3.44 "
60.30604	2.109	E-3 0.207	13.82 "	-4.35 "
60.43478	2.444	E-3 0.386	12.97 "	1.32 "
61.15057	2.486	E-3 0.621	12.48 "	-0.36 "
61.80017	2.281	E-3 0.910	12.07 "	-1.59 "
62.41122	1.919	E-3 1.255	11.71 "	-2.66 "
62.48626	1.507	E-3 0.0827	14.68 "	-5.03 "
62.99800	1.492	E-3 1.66	11.39 "	-3.34 "
63.56854	1.079	E-3 2.11	11.08 "	-4.17 "
64.12778	7.281	E-4 2.62	10.78 "	-4.48 "
64.67892	4.601	E-4 3.19	10.5 "	-5.1 "
65.22408	2.727	E-4 3.81	10.2 "	-5.1 "
65.76474	1.52	E-4 4.48	10.0 "	-5.7 "
66.30206	7.94	E-5 5.22	9.7 "	-5.5 "
66.83677	3.91	E-5 6.00	9.4 "	-5.9 "
67.36951	1.81	E-5 6.84	9.2 "	-5.6 "
67.90073	7.95	E-6 7.74	8.9 "	-5.8 "
68.4308	3.28	E-6 8.69	8.7 "	-5.7 "
118.75034	9.341	E-4 0.0138	15.92 "	-0.44 "



30

Figure 3-3. Contours of average absolute humidity ( $\text{g/m}^3$ ) for a summer month (August for the northern hemisphere and February for the southern hemisphere) (Bean and Dutton, 1966).

To calculate water vapor absorption per unit length,  $\alpha_2$ , to 50 GHz:

$$\alpha_2 = 0.1820 f \left[ \sum_{b=1}^6 S_b F_b'' \right] + 0.1820 f N_w'' \quad (3-11)$$

$$S_b = B_1 p_w t^{3.5} \exp [B_2(1 - t)] \quad (\text{see Eq. 3-8}) \quad (3-12)$$

$$F_b'' = \frac{f \gamma_b}{f_b} \left( \frac{1}{(f_b - f)^2 + \gamma_b^2} + \frac{1}{(f_b + f)^2 + \gamma_b^2} \right) \quad (3-13)$$

$$\gamma_b = B_3 (p + 4.80 p_w) t^{0.6} \quad (3-14)$$

$$N_w'' = 1.87 \times 10^{-5} p p_w t^{3.1} f. \quad (3-15)$$

For values of  $f_b$ ,  $B_1$ ,  $B_2$ ,  $B_3$ , and  $B_4$ , see Table 3-2.

TABLE 3-2. WATER VAPOR LINES

$f_b$	$B_1$	$B_2$	$B_3$	$B_4$
22.23508	0.112	2.143	$28.1 \times 10^{-3}$	0
68.052	0.018	8.75	28 "	0
183.31009	2.41	0.653	28.2 "	0
321.22564	0.044	6.16	22 "	0
325.15292	1.59	1.52	29 "	0
380.19737	12.40	1.02	28.5 "	0

Table 3-3 is an example of the output format for Program No. 3. The primary output is one number (the estimate of median basic transmission loss). The median basic transmission loss is estimated by adding  $L_{bf}$  and  $A_\alpha$  as was done in MIL-HDBK-416 (1977). Using this value, Program No. 4 will calculate the time distributions of basic transmission loss due to rain and multipath.

Table 3-3. Example of the Tabular Output Format From  
the Median Basic Transmission Loss Model

Median Basic Transmission Loss for the  
Path from LANGERKOPF to FELDBERG

(June 8, 1978 - Project No: 9103504 - DRW)

Path Length	=	114.55 km
Carrier Frequency	=	8.20 GHz
Mean Path Temperature	=	20.0 C
Mean Path Pressure	=	95.07 kPa
Mean Absolute Humidity	=	12.00 g/cu m

-----

Free Space Basic Transmission Loss	=	151.91 dB
Oxygen Absorption Loss	=	0.73 dB
Water Vapor Absorption Loss	=	0.64 dB
		-----
Total Median Transmission Loss from LKF to FEL	=	153.27 dB

-----

(Program Version: 17May78)

#### PROGRAM NO. 4, PATH-LOSS VARIABILITY MODEL

There are essentially two components of temporal path-loss variability that can be estimated in a quantitative way. These components are multipath fading and rain attenuation and they appear in the path-loss variability flow diagram in Figure 4-1. There are other causes of path-loss variability besides these two mechanisms but for a line-of-sight (LOS) microwave path designed with proper antenna characteristics and sufficient terrain clearance, these other causes are of less importance. Two of these mechanisms are defocusing and diffraction fading.

In MIL-HDBK-416 (1977), the Barnett model was used for multipath effects. In the automated digital system engineering model, we use an updated version of the Barnett model which appears in an article by A. Vigants (1975) entitled "Space-Diversity Engineering". This model for calculating multipath effects on LOS systems has become widely accepted for paths between 20 and 60 km long. For long paths, we used the Japanese model, Morita (1970). This model was developed from a data base including much longer paths than the Barnett model included.

One year of data for 5 GHz paths across the English Channel (88 km from Swingate, England to Houtem, Belgium) has recently been obtained. This set of data is useful for comparison with long LOS multipath attenuation models. The data set indicates that the temporal distribution of signal levels (Figure 4-2) was much less severe than would be predicted from a simple extension of the Barnett model. Barnett (1972), pages 332-333, states reasons why the Barnett model should not be extended in a simple manner to long paths.

Analysis of the Swingate-Houtem data indicates that the multipath model may relax to a Rayleigh distribution as path length increases. This Rayleigh distribution can be expressed as follows:

$$P = 1 - \exp \left\{ -\ln 2 \cdot 10^{-M_f/10} \right\} \quad (4-1)$$

where P is the fraction of time during which the signal is  $M_f$  dB or more below the long-term median.

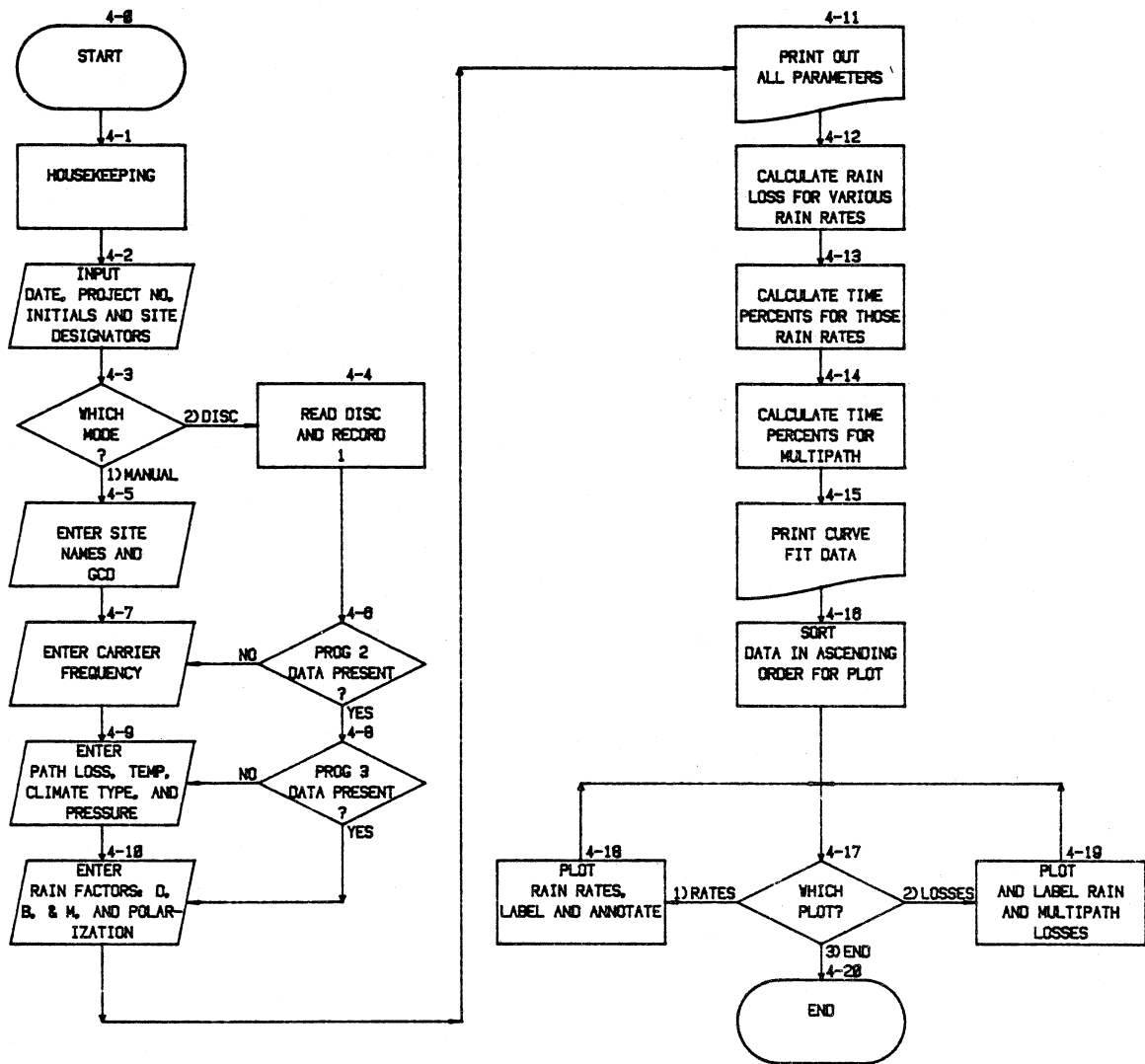


Figure 4-1. Path Loss Variability Model.

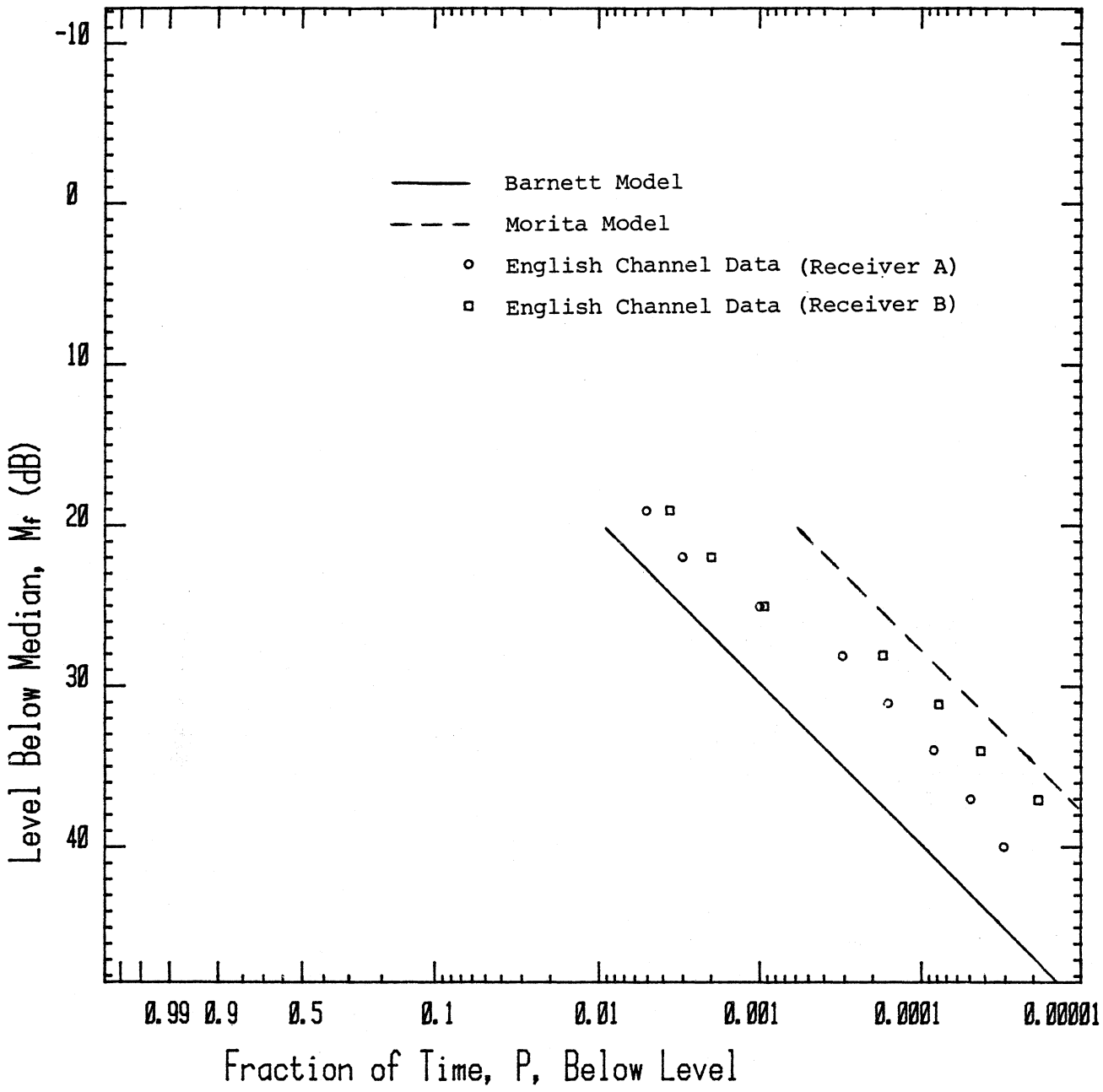


Figure 4-2. Comparison of prediction methods with one year of data from an LOS path across the English Channel (88 km, 5 GHz).

The Barnett model may be presented in the following form:

$$P_m = 0.24(c) \left(\frac{f}{4}\right) (d^3) (10^{-5}) 10^{-M_f/10}, M_f > 20 \quad (4-2)$$

where

$$0.24(c) \left(\frac{f}{4}\right) (d^3) (10^{-5}) < 1$$

$P_m$  = the fraction of time that the signal fades to a depth greater than  $M_f$  during the worst fading month.

$M_f$  = the fade depth exceeded referred to the median signal level in dB.  $M_f > 20$ .

$d$  = the path length in km.  $15 < d < 50$ .

$f$  = the frequency in GHz.  $1 < f < 50$ .

$c$  = the climate factor

1 average terrain  
 $c = 4$  over-water and coastal areas  
 0.25 mountains and dry climate

The Morita model presented in Morita (1970), page 810, predicts the fraction of time that a microwave path is in a Rayleigh fading mode. A translation of this model in terms of the same  $P$ ,  $d$ ,  $f$ , and  $M_f$  as the Barnett model may be written as follows:

$$P_m = Q \left(\frac{f}{4}\right)^{1.2} (d^{3.5}) (1 - \exp \{-\ln 2 / 10^{M_f/10}\}) \quad (4-3)$$

where

$$Q \left(\frac{f}{4}\right)^{1.2} (d^{3.5}) < 1$$

$Q = 2 \times 10^{-9}$  over mountains  
 $Q = 5.1 \times 10^{-9}$  average terrain  
 $Q = 3.7 \times 10^{-7} (1/h)^{0.5}$  over water and coastal areas

$h$  = average path height above ground in meters.  $d > 50$ .

Of all models for multipath fading, the Barnett and Morita models have the largest data bases and seem to us to have been more carefully thought out and checked than any other models. For these two reasons they have been selected for inclusion in the automated digital system engineering model.

To convert the average fraction of time below a given level  $P_m$  during the worst fading month to the fraction of time below a given level during an average year,  $P_y$ , the method described by Vigants (1975) is recommended. This procedure is given by the equation:

$$P_y = P_m (9T_o + 160) \times 10^{-3} \quad (0 < T_o < 25) \quad (4-4)$$

where  $T_o$  is the mean annual temperature in degrees Celsius (C) on the ray path.

Figure 4-3 shows the estimated time variability of basic transmission loss due to multipath alone and rain attenuation alone. This figure is the format of the main output of Program No. 4. From this presentation, the relative importance of multipath and rain attenuation fading with respect to each other is quickly apparent. Table 4-1 is an example of the tabular format for showing much the same information as Figure 4-3. This format is the most convenient type for transmitting the information needed for manual entry into Program No. 5.

To calculate the time below a given level referenced to the long-term median due to rain attenuation, the Rice-Holmberg (R-H) model will be used (Rice and Holmberg, 1973). The techniques and refinements of the R-H model developed for Europe (Dutton, et al., 1974) and for the United States (Dutton, 1977) will be used in the model. The Rice-Holmberg algorithm is as follows:

The R-H model determines the number of hours in an average year of rainy  $t$ -minute periods,  $T_t(R)$ , for which a surface rain rate,  $R$ , in mm/hr is expected to be exceeded. The value  $T_t(R)$  is given in the R-H model (continuing their notation) as

$$T_t(R) = T_{1t} q_{1t}(R) + T_{2t} q_{2t}(R) \text{ hrs,} \quad (4-5)$$

where

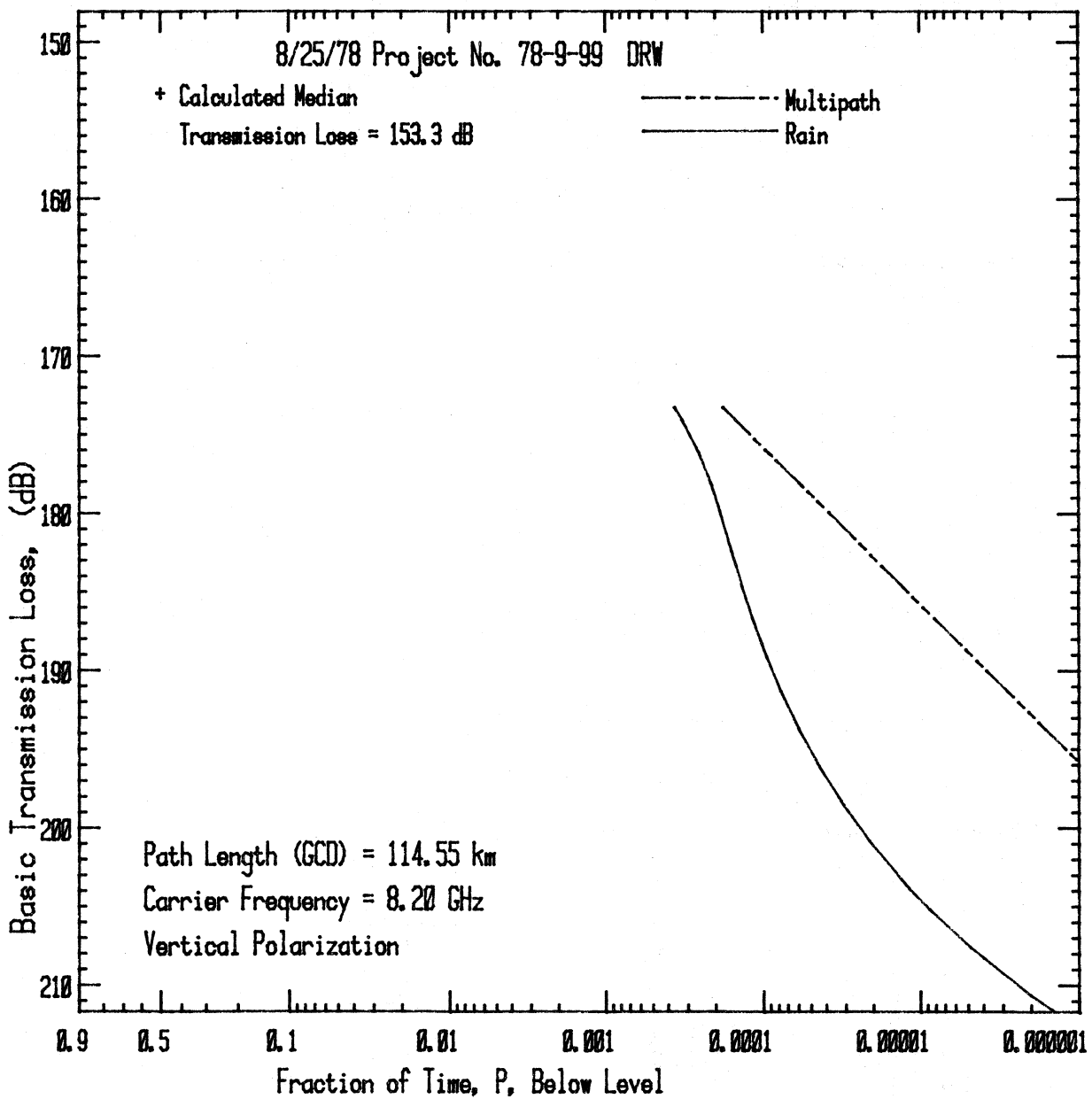
$$q_{1t}(R) = \exp(-R/\bar{R}_{1t}), \quad (4-6)$$

$$q_{2t}(R) = 0.35 \exp(-0.453074R/\bar{R}_{2t}) + 0.65 \exp(-2.857143R/\bar{R}_{2t}), \quad (4-7)$$

$$T_{1t} = \beta M/\bar{R}_{1t} \text{ hrs,} \quad (4-8)$$

$$T_{2t} = (1-\beta)M/\bar{R}_{2t} \text{ hrs,} \quad (4-9)$$

where  $M$  is the recorded station average annual precipitation in millimeters and  $\beta$  is the ratio of "thunderstorm rain",  $M_1$ , to  $M$  for a year.



Terrain type = mountains  
Avg. Annual Temp. = 20 °C

Radome Loss per Antenna = 1.6 dB  
Mean Annual Rainfall = 800 mm  
No. of Rainy Days/yr. = 111  
Thunderstorm Ratio B = 0.15

Multipath and Rain Loss Variability  
for the Path from FELDBERG  
Tower 0 to LANGERKOPF Tower 1

Figure 4-3. Example basic transmission loss variability distributions.

Table 4-1. Example of Tabular Output of Path Loss Variability Information

Multipath and Rain Loss Variability  
for the FELDBERG, LANGERKOPF Link

8/25/78 Project No. 78-9-99 DRW

Transmitter:		FEL 0
Receiver:		LKF 1
Path Length - G.C.D. (km)	=	114.55
Frequency (GHz)	=	8.20
Vertical Polarization		
Median Transmission Loss (dB)	=	153.27
Avg annual Temperature (C)	=	20
No. Rainy Days/Year	=	111
Annual Precipitation (mm)	=	800
Thunderstorm ratio: Beta	=	0.15
Terrain factor (mountains )	=	0.25

-----  
Rain attenuation curve:

Transmission loss (dB)	Loss below Median(dB)	Fraction of time, P, Loss is exceeded
173.3	20.0	3.64E-04
178.3	25.0	2.11E-04
183.3	30.0	1.49E-04
188.3	35.0	1.02E-04
193.3	40.0	6.25E-05
198.3	45.0	3.23E-05
203.3	50.0	1.32E-05
208.3	55.0	3.99E-06
213.3	60.0	8.22E-07

-----  
Multipath equation:

Multipath coefficient,  $K = 0.02589$   
 $P = K * [1 - \exp(-\ln 2 / X)]$ , where  $X = 10^{(0.1 * M)}$   
 and  $M =$  Number of dB below median loss.

-----  
(Program Version: 25Aug 78)

$$\bar{R}_{1t} = A_1 + B_1 \ln \left\{ C_1 \exp \left[ \frac{-30}{t+10} \right] + \frac{1}{t+10} \right\} \text{ mm/hr,} \quad (4-10)$$

$$A_1 = 1 + 65.67864 \exp(-\beta M / 8766) \text{ mm/hr,} \quad (4-11)$$

$$B_1 = 13.457 \exp(-\beta M / 8766) \text{ mm/hr,} \quad (4-12)$$

$$C_1 = 0.00704709132, \quad (4-13)$$

$$\bar{R}_{2t} = \frac{(1-\beta)M}{24D[0.165 + 0.776 \exp(-120/t) + A \exp(-B/t)]} \text{ mm/hr.} \quad (4-14)$$

Here  $D = D(0.01)$  is the number of days during an average year in which precipitation exceeded 0.01 inches of recorded precipitation, and

$$B = 1443.95 \ln \left[ 8.26136 \left( \frac{365.25}{D} - 0.940823 \right) \right] \quad (4-15)$$

$$A = \frac{\exp(B/1440)}{8.26136}. \quad (4-16)$$

We are interested in rain rate events of very short duration and therefore chose  $t = 1$ . The value of  $D$  for Europe is found by using

$$D = 0.07651M - 83.632\beta + 62.523. \quad (4-17)$$

The unknowns in the equations 4-5 through 4-17 are  $\beta$ ,  $M$ , and  $D$ . Many of these values are obtained from Figures 4-4 through 4-10. The figures show values of  $\beta$  and  $M$  for Europe, the United States and roughly estimated values for the remainder of the world. For parts of the world other than the U.S. and Europe, a value for  $M$  can be obtained from The Times Atlas of the World (1975) plate 4. For parts of the world other than the U.S. and Europe,

$$D = 1 + M/8 \text{ or } D = 365 \quad (4-18)$$

whichever is less. For most of the world measured statistics are not available for  $D$  necessitating the approximations provided by eqs. 4-17 and 4-18.

A special map of annual rainfall throughout the world is often needed when using Program No. 4. This large map is provided in the computer operators manual since the model is very sensitive to this parameter. The world maps should only be used outside the United States and Europe.

Figure 4-11 is an example output of the point rain rate distribution. This computer output is useful to the engineer evaluating a long path traversing more than one rainfall value region. The fraction of time,  $P$ , that a given rain rate is exceeded on this graph is obtained from the equation:

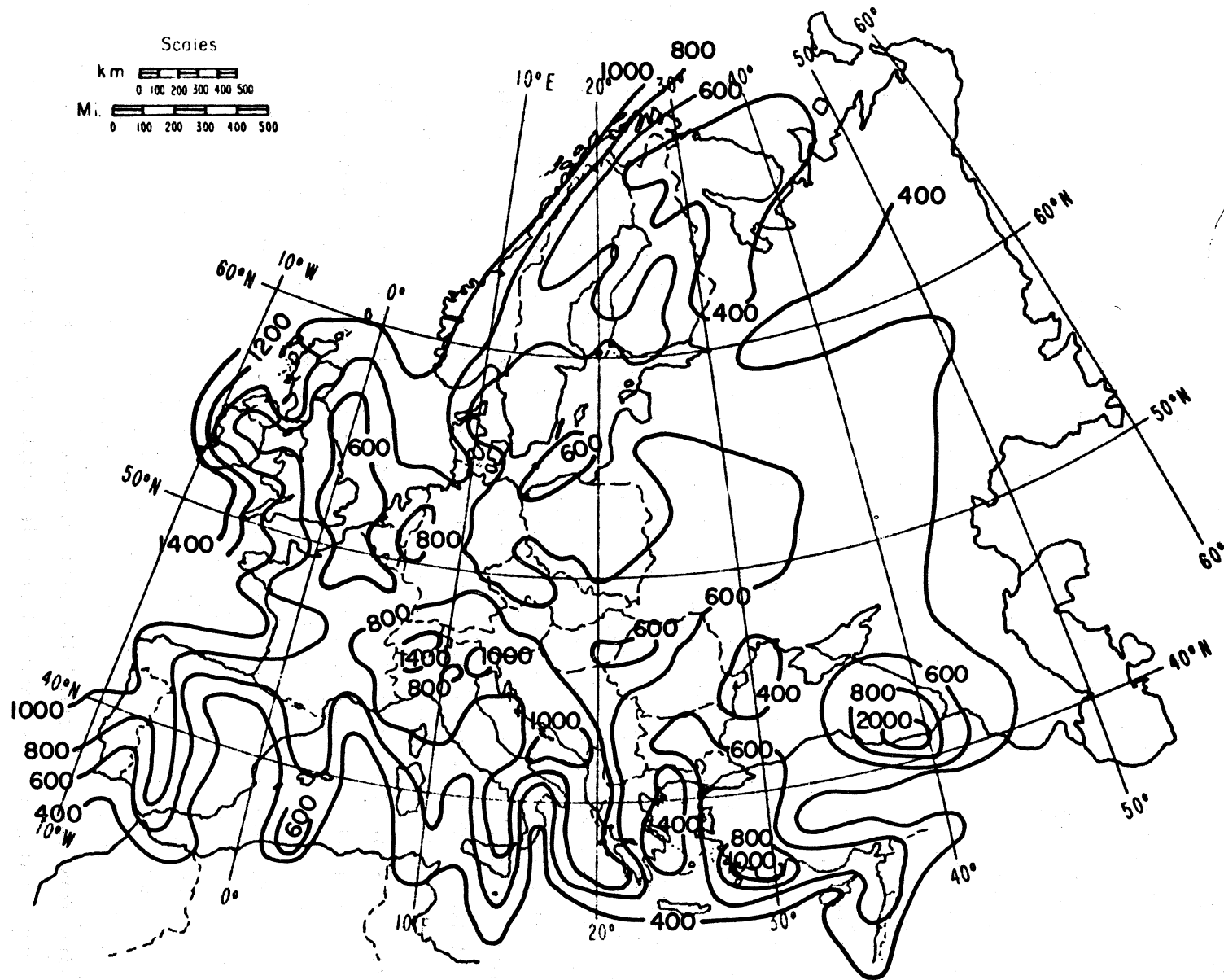
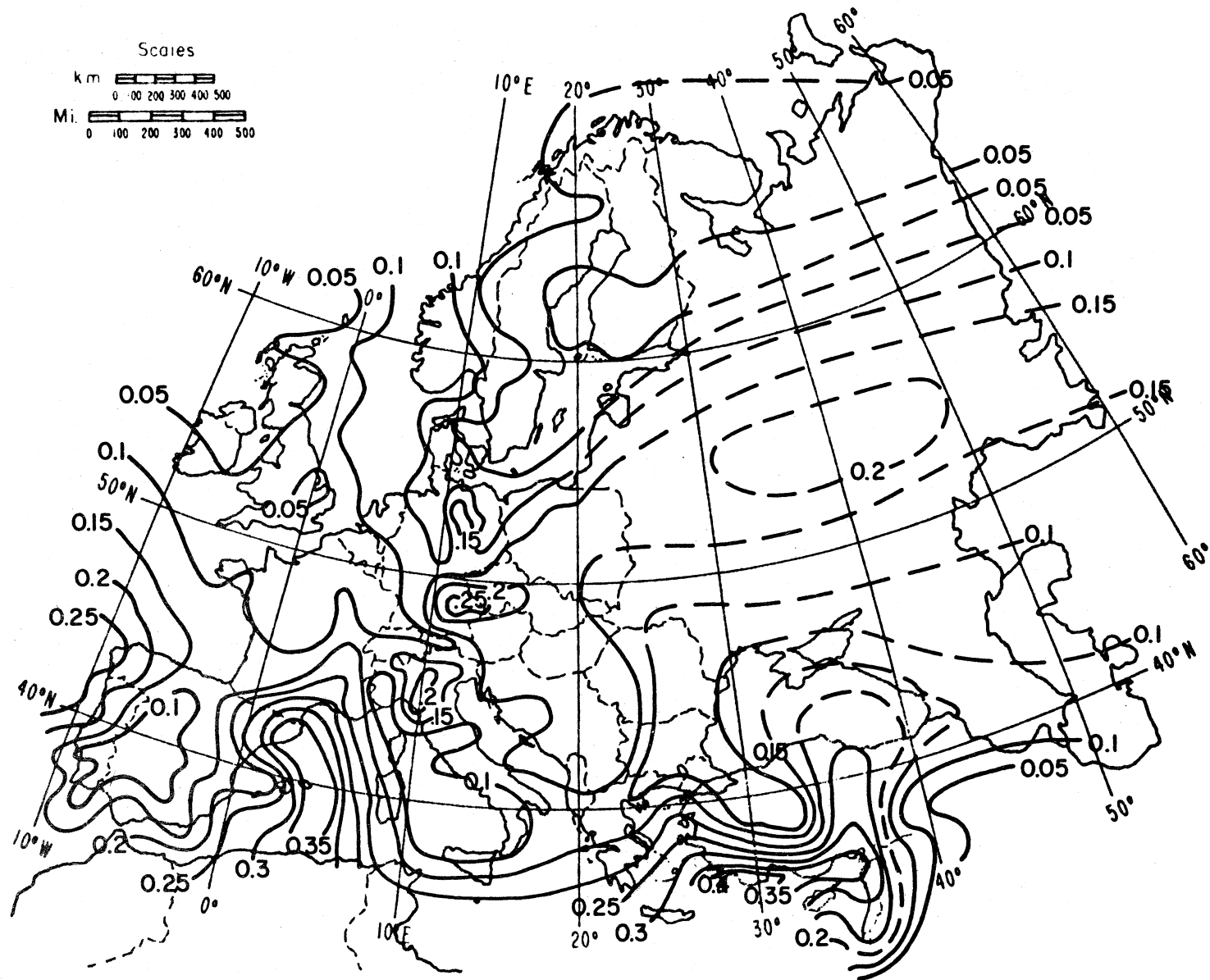


Figure 4-4. Annual precipitation, M, in millimeters, for an average year in Europe.



42

Figure 4-5. Mean annual thunderstorm ratio,  $\beta$ , for Europe. (Dashed contours indicate regions of sparse data.)

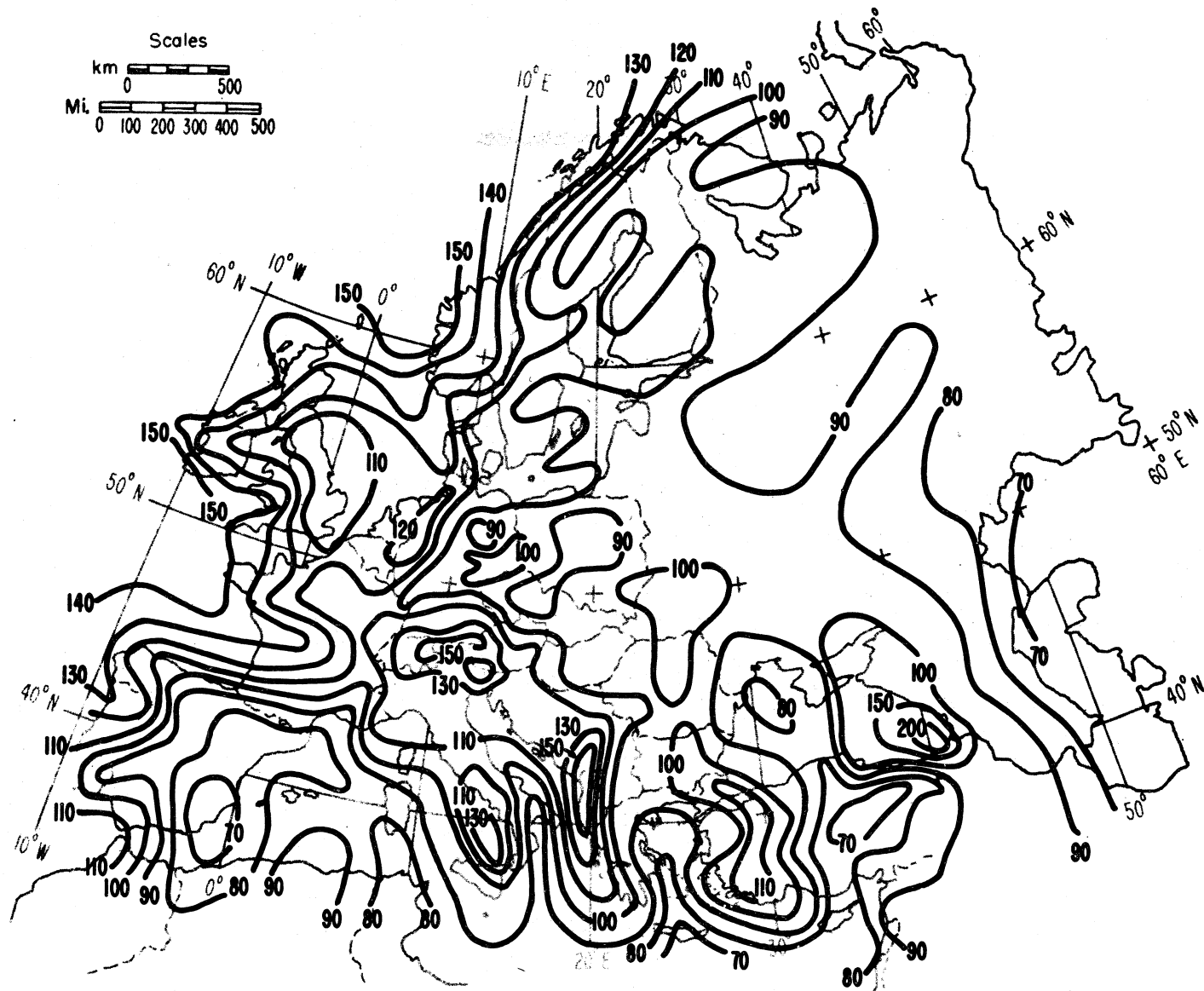


Figure 4-6. The estimated number of rainy days,  $D$ , for an average year in Europe.

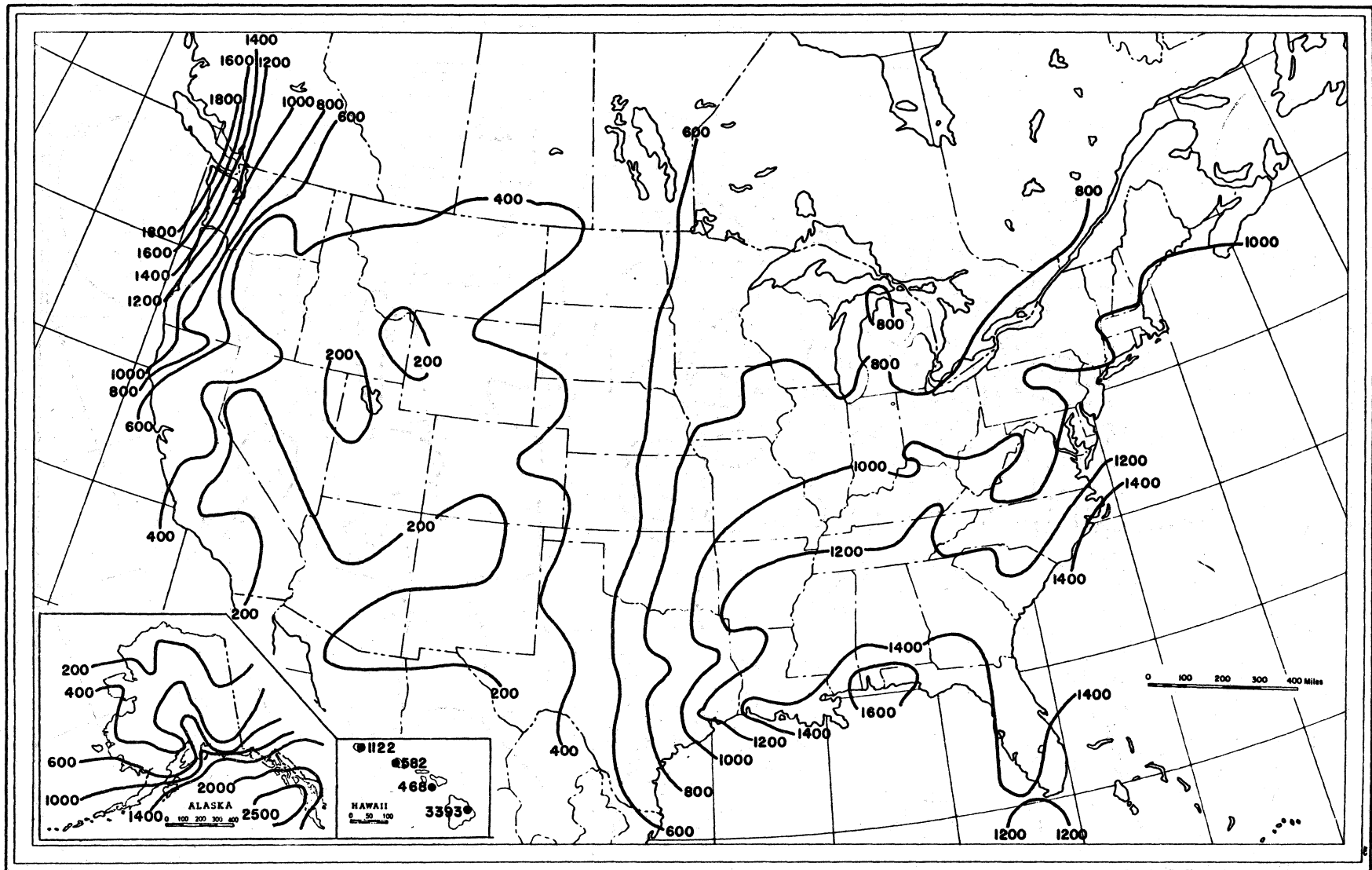


Figure 4-7. 30-year mean annual precipitation,  $M$ , in millimeters, for the U.S.A.

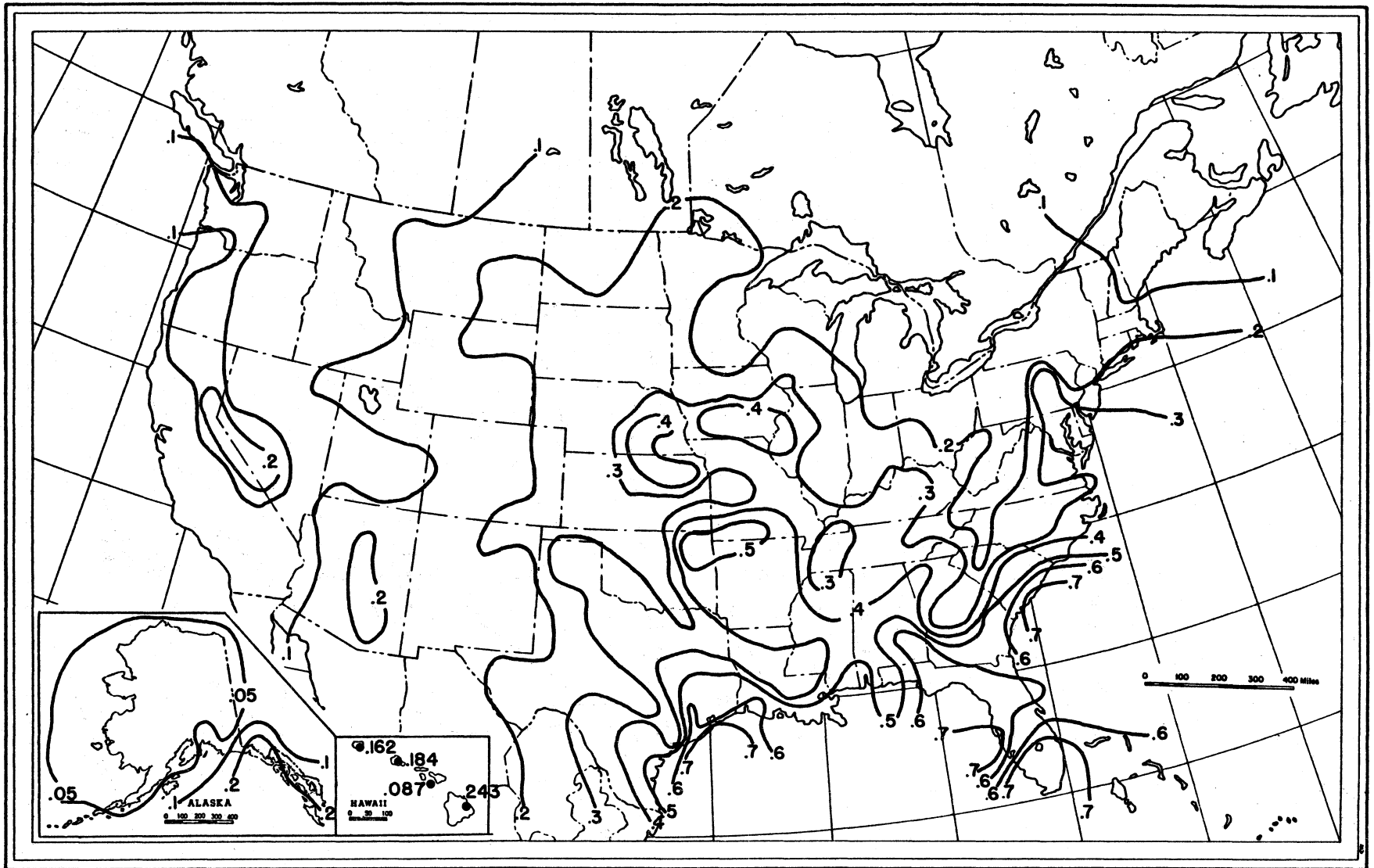


Figure 4-8. Mean annual thunderstorm ratio,  $\beta$ , for the U.S.A.

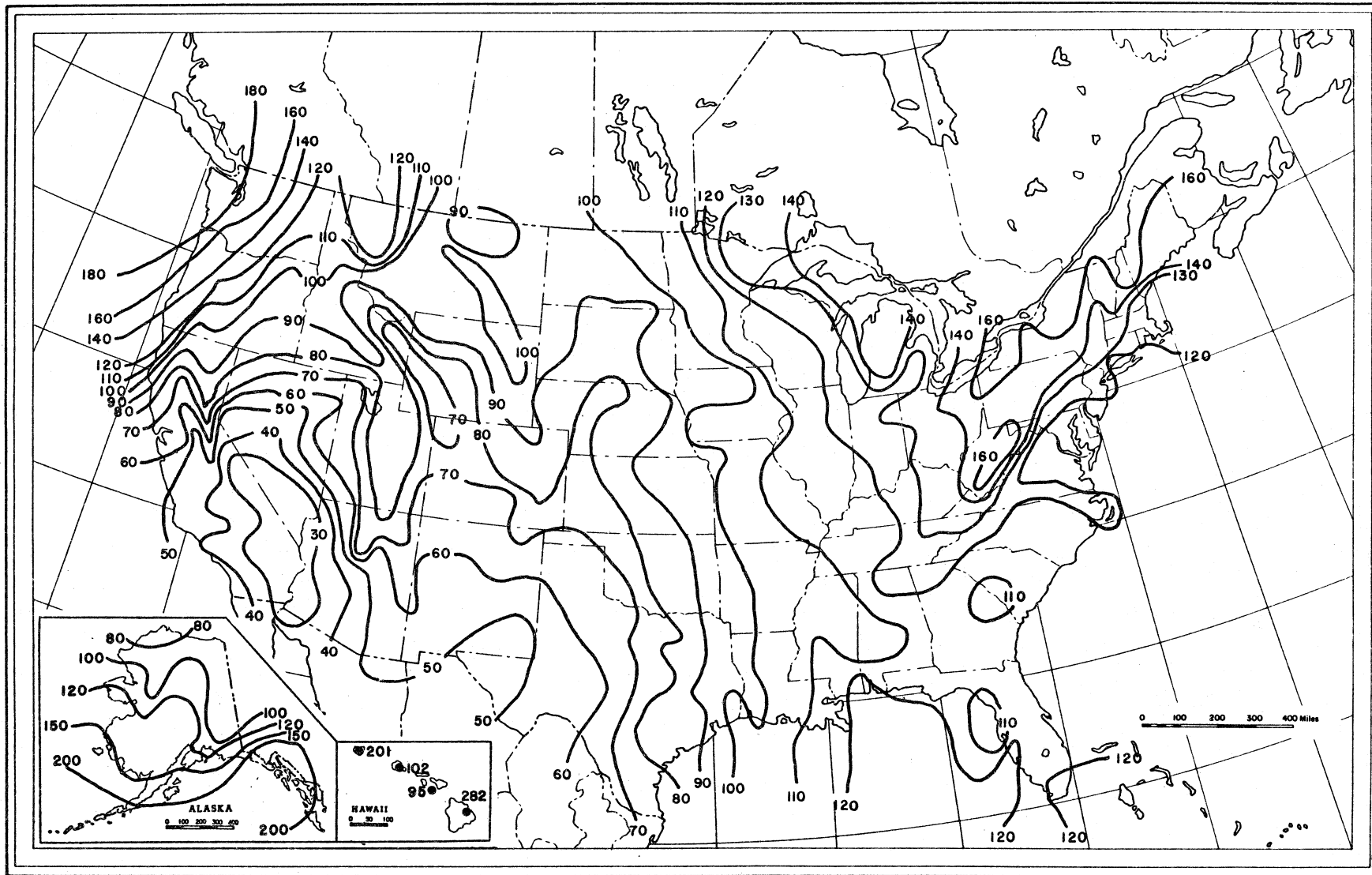


Figure 4-9. 30-year annual number of days,  $D$ , with precipitation greater than 0.25 mm for the U.S.A.

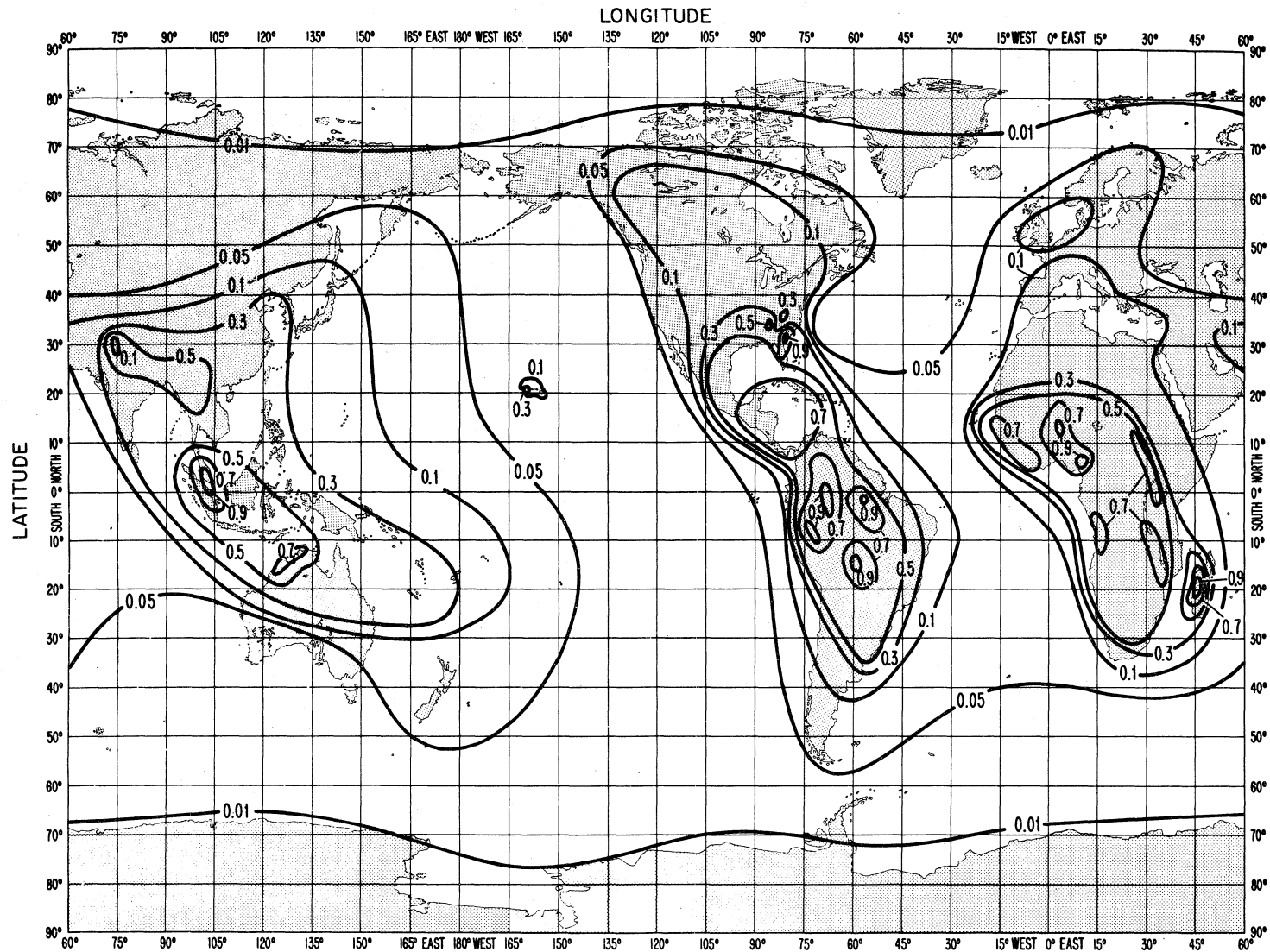
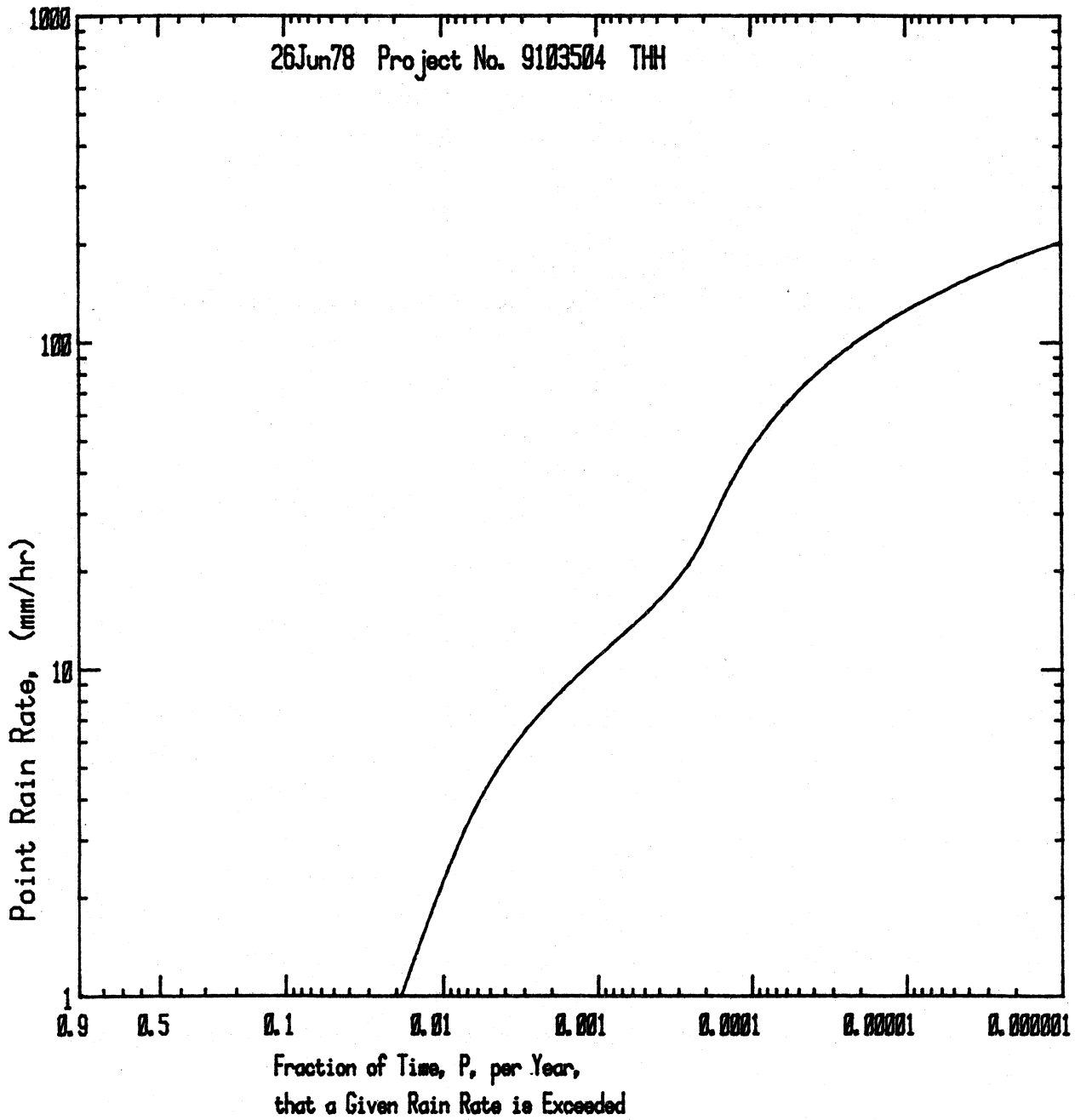


Figure 4-10. Mean annual thunderstorm ratio,  $\beta$ , for the world.

26Jun78 Project No. 9103504 THH



Mean Annual Rainfall = 800 mm  
No. of Rainy Days/yr. = 111  
Thunderstorm Ratio B = 0.15

Point Rain Rate Time Distribution  
for the Path from FELDBERG  
Tower 0 to LANGERKOPF Tower 1

Figure 4-11. Example point rain rate distribution.

$$P = T_t(R)/8766. \quad (4-19)$$

The layer of water formed on an antenna weather cover during a rain storm produces a few dB of attenuation (Hogg et al., 1977, pp. 1579).

The amount of attenuation depends on several factors:

1. Rain rate
2. Wind direction
3. Condition of the radome surface; i.e., roughness, weathering, composition, etc.
4. The shape of the radome, i.e., flat or curved.
5. The microwave frequency.

Measurements produced 4 to 8 dB attenuation at 20 GHz and 3 to 6 dB at 11 GHz (Hogg et al., 1977). An equation for estimating radome attenuation,  $A_w$ , for each antenna is:

$$A_w = 0.2 f \quad 5 < f < 50 \text{ GHz} \quad (4-20)$$

where  $f$  is the carrier frequency in GHz and  $A_w$  is the wet radome attenuation in dB.

This estimate is for a parabolic antenna with a flat weather cover.

CCIR (1974a) shows the calculation of attenuation per unit path length due to rain as a function of radio frequency and rain rate. It has become clear that the polarization of the radio wave is also an important variable (Hogg, et al., 1977, pp. 1577-1578). The relationship between rain attenuation,  $\gamma_{H,V}$  for spherical raindrops, and rain rate and frequency may be expressed as follows:

$$\gamma_{H,V} = K_{H,V} R^\alpha \text{ dB/km} \quad (4-21)$$

where  $K$  and  $\alpha$  are functions of frequency and  $R$  is the rain rate in mm/hr (CCIR, 1974a, pp. 71).

$$\alpha = -0.0059 f + 1.265 \quad 5 < f < 50 \text{ GHz} \quad (4-22)$$

These expressions for  $\alpha$  and  $K$  are obtained from measured values (Lin, 1977, pp. 1597) and (CCIR, 1974a, pp. 77)  $f$  is the carrier frequency in GHz.

$$K_H = \left( \frac{f - 4.5}{190} \right)^{(-0.0059 f + 1.265)} \quad 5 < f < 50 \text{ GHz} \quad (4-23)$$

Using the experimental results on attenuation polarization dependence described by Hogg, et al. (1977):

$$\gamma_H = \left( \frac{f - 4.5}{190} \times R \right)^{(-0.0059 f + 1.265)} \quad (4-24)$$

for horizontal polarization and

$$\gamma_V = \left( 0.84 + \frac{0.34}{f-2.9} \right) \gamma_H \quad 5 < f < 50 \text{ GHz} \quad (4-25)$$

for vertical polarization.

If the rain rate along a path were uniform, the total path attenuation,  $A_R$ , would be equal to  $A_W$  plus the length of the path,  $d$ , times  $\gamma_{H,V}$ . High rain rates are not uniformly distributed along paths longer than a few hundred meters, therefore an expression is required to relate point rain rate to path rate. A simple expression for the ratio of path rate,  $R_{PA}$ , to point rate,  $R$ , is given in Lin (1977) and it has been checked against measured data,

$$\frac{R_{PA}}{R} = \frac{2636}{2636 + d (R - 6.2)} \quad R > 10 \text{ mm/hr.} \quad (4-26)$$

To calculate total path attenuation due to rain,

$$A_R = A_W + \frac{\gamma_{H,V} d 2636}{2636 + d (R - 6.2)} \quad R > 10 \text{ mm/hr.} \quad (4-27)$$

The variability of path loss due to rain attenuation is plotted using the graphical format shown in Figure 4-3. The basic transmission loss,  $L_b$ , shown for rain in this figure is approximately equal to the median basic transmission loss added to the rain attenuation,  $A_R$ .

PROGRAM NO. 5, LINK EQUIPMENT GAIN

In order to assess adequately the performance of a microwave link, it is necessary to calculate the time availability distribution of received signal level, RSL, at each end of the link. To calculate this distribution, information on the following considerations is required:

1. Median basic transmission loss across the path.
2. Variability of the transmission loss.
3. Antenna gains.
4. Transmitter power output.
5. Transmission line loss.
6. Diplexer and power splitter losses.
7. Type and configuration of the diversity and combining system.
8. Equipment and support systems reliability.

Calculation of equipment and support system reliability is generally considered separately from the other seven components. Usually a given amount of allotted outage time is assigned to equipment and support systems failure and approximately the same amount of time is assigned to anomalies associated with the propagation path. Program No. 5 calculates the time availability of RSL assuming uninterrupted equipment and support system service. A simplified flow diagram of the Link Equipment Gain program is presented in Figure 5-1.

Basic transmission loss and its variability is calculated in programs 3 and 4.

Antenna gains for parabolic antennas may be supplied to the program either by direct entry or by entering carrier frequency and aperture diameter. To calculate antenna gain,  $G$ , we use the equation from MIL-HDBK-416 (1977), page 4-194:

$$G = 10 \log \frac{\eta \pi^2 D^2}{\lambda^2} \text{ dBi} \quad (5-1)$$

where

$\eta$  = aperture efficiency (usually 0.55),

$D$  = diameter;  $\lambda$  = wavelength (in the same units).

Equation 5-1 may be rewritten for  $\eta = 0.55$ ,  $f$  in GHz and  $D$  in meters to give:

$$G = 20 \log 7.772 Df \text{ dB.} \quad (5-2)$$

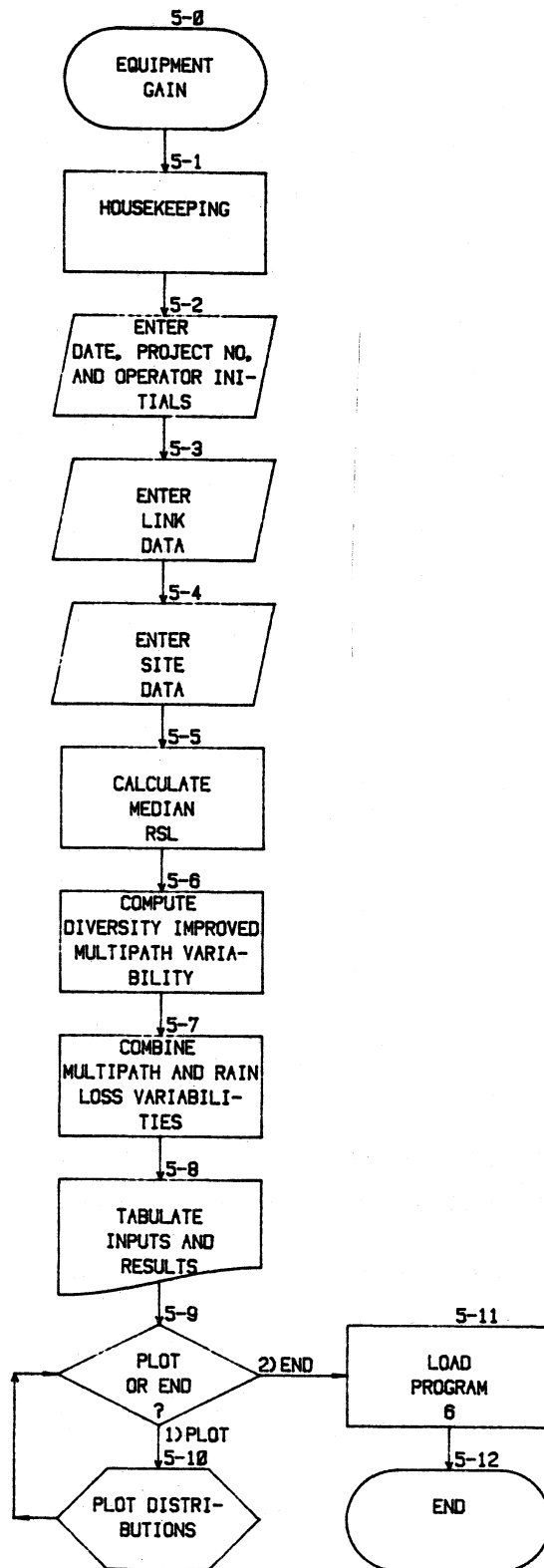


Figure 5-1. Link equipment gain.

Transmitter power output is entered in dB above a milliwatt (dBm). (One Watt is equal to +30 dBm.) Transmission line loss values may be entered directly or values may be calculated from line lengths and from graphs provided in the Andrew Systems Catalog (1978) (Figure 5-2).

Diplexer losses should be entered when they are applicable (applicability depends upon where receiver and transmitter power measurement reference points are located in the system).

Calculation of vertical space diversity improvement,  $I_{os}$ , (with switch combining) is based on the model provided by Vigants (1975) pp. 110-112. If we let  $T_m$  be the time that the signal from the main antenna remains below a given signal level and if we let  $T_s$  be the simultaneous time that the signal from both antennas is below L, then  $I_{os}$  is defined as  $T_m/T_s$ . From Vigants' (1975) model,

$$I_{os} = 0.001213 \frac{f s^2}{d} \times 10^{\frac{(G_s - G_m + M_f)}{10}}, \quad \begin{matrix} s < 20 \\ M_f > 20 \end{matrix} \quad (5-3)$$

where

$G_m$  = the median RSL from the main antenna in dBm

$G_s$  = the median RSL from the secondary antenna in dBm

$f$  = the carrier frequency in GHz

$s$  = the vertical separation of antennas in meters, center-to-center

$d$  = the path length in kilometers

$M_f$  = the fading depth below the median RSL

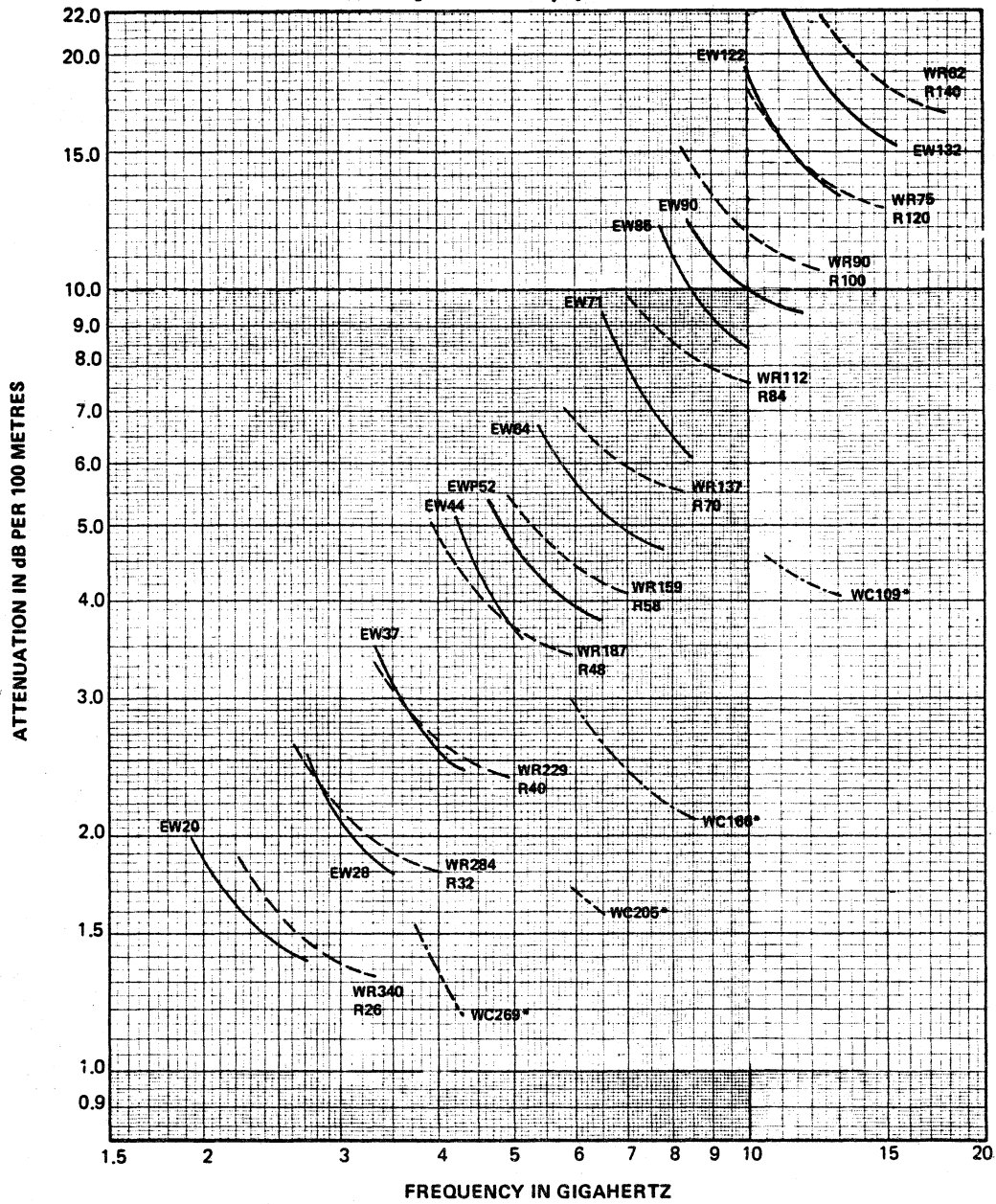
For calculating frequency diversity improvement,  $I_{of}$ , we also use the model given in Vigants (1975):

$$I_{of} = 80.47 \frac{|f_1 - f_2|}{f_1^2 d} \times 10^{M_f/10}, \quad \begin{matrix} |f_1 - f_2| < 0.5 \\ M_f > 20 \end{matrix} \quad (5-4)$$

where

$f_1$  and  $f_2$  are the carrier frequencies in GHz.

Reproduced by permission of ANDREW Corp.



Attenuation curves based on:  
VSWR 1.0  
Ambient Temperature 24°C (75°F)  
High-Conductivity Copper

Figure 5-2. Microwave waveguide attenuation.

The value of  $I_o$  calculated in equations 5-2 and 5-4 is valid only if the diversity signal is at each instant the stronger of the two received signals. If switching only occurs when the receiver off-line has a signal level which exceeds the on-line receiver signal by some threshold power ratio, B, in dB, the actual diversity improvement is I where:

$$I = \eta_d I_o. \quad (5-5)$$

The efficiency factor,  $\eta_d$  is given by:

$$\eta_d = 2 \left( 10^{B/10} + 10^{-B/10} \right)^{-1}. \quad (5-6)$$

For example if B = 6 dB,  $\eta_d = 0.47$ . Such threshold power ratios for switching are often built into combiner configurations to prevent excessive switching.

Table 5-1 is a sample summary of the link and equipment parameters used to calculate RSL. This summary is one of the two output formats from Program No. 5. Figure 5-3 is a sample of the time availability distribution output format. The RSL distribution without diversity (Figure 5-3) is obtained by combining RSL variability due to rain attenuation with the variability due to multipath without diversity. The combining of variability distributions is done by adding the fraction of time below a given level due to multipath to the fraction of time below the same level due to rain. To obtain the RSL distribution with diversity (Figure 5-3), the multipath variability with diversity must be calculated using the diversity improvement factor, I. Diversity is only an aid for decreasing the effect of multipath fading. The distributions of the rain signal level and the diversity improved multipath signal are combined in the same manner as they were in the nondiversity case. In our calculations, we assume that for frequency diversity the difference in carrier frequency values is negligibly small in terms of the effects on median signal level and variability. The distributions can be combined by simply adding the times below a given level because, in general, multipath fading does not occur at the same time as rain attenuation fading.

Table 5-1. Sample Summary of Basic Link and Equipment Gain Parameters

Basic Path and Equipment Gain Parameters for the Link  
from FELDBERG to LANGERKOPF (Sheet 1)

(18Jul78 Project No. 9103504 THH)

<u>Input Parameter</u>	<u>Transmitter</u>	<u>Receiver</u>	
		<u>Primary</u>	<u>Secondary</u>
Site Designator	= FEL		LKF
Tower Number	= 0		1
Latitude	= 50 14'33.00"N	49 18' 4.00"N	
Longitude	= 8 29'49.00"E	7 50'47.00"E	
Tower Base Elev. above MSL (m)	= 688.80	602.00	
Azimuth from True North	=204 18' 1.69"	23 48'13.55"	
Azimuth from Magnetic North	=192 15'	11 41'	
Antenna Height above Ground (m)	= 120.00	105.00	90.00
Antenna Type	= PARABOLIC	PARABOLIC	PARABOLIC
Antenna Gain (dBi)	= 47.36	47.36	47.36
Antenna Diameter (m)	= 3.66	3.66	3.66
Feeder Type	= EW85	EW85	EW85
Feeder Loss (dB/100m)	= 10.50	10.50	10.50
Feeder Length (m)	= 135.00	120.00	115.00
Total Line Loss (dB)	= 14.18	12.60	12.08
Circulator/Diplexer Loss (dB)	= 1.00	1.20	1.00

Table 5-1. Sample Summary of Basic Link and Equipment Gain Parameters

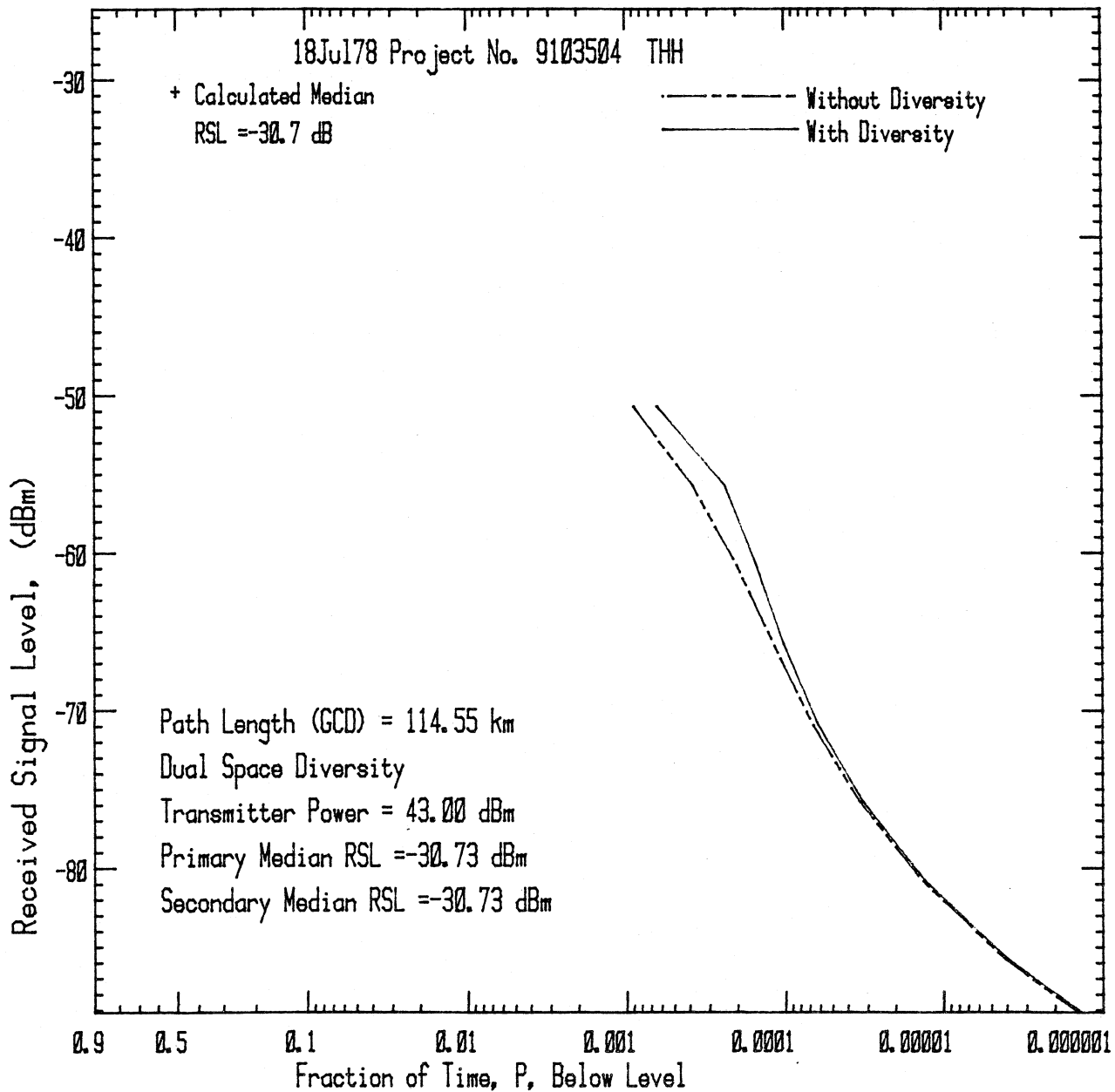
Basic Path and Equipment Gain Parameters for the Link  
from FELDBERG to LANGERKOPF (Sheet 2)

Path Length	(km) =	114.55
Polarization	=	Vertical
Primary Carrier Frequency	(GHz) =	8.20
Receiver Front-End Type	=	PREAMP20DB
Receiver Front-End Location	=	ANTENNA
Diversity Configuration	=	DUAL SPACE
Detection Combiner Type	=	PRE DETEC
Combiner Type	=	MAX RATIO
Transmitter Power	(dBm) =	43.00
Median Basic Transmission Loss	(dB) =	153.27
Primary Receiver Median RSL	(dBm) =	-30.73
Secondary Receiver Median RSL	(dBm) =	-30.73
Vertical Antenna Separation	(m) =	15.00
Difference in Median RSL	(dB) =	0.00
Diversity Efficiency Factor	=	1.00

-----  
Received Signal Level Curve:

Received Signal Level: RSL (dBm)	RSL Below Median (dB)	Space Diversity Improvement	Fraction of time, P, below RSL
-50.7	20.0	2.0	6.33E-04
-55.7	25.0	6.2	2.38E-04
-60.7	30.0	19.5	1.52E-04
-65.7	35.0	61.8	1.02E-04
-70.7	40.0	195.4	6.25E-05
-75.7	45.0	617.9	3.23E-05
-80.7	50.0	1954.0	1.32E-05
-85.7	55.0	6179.2	3.99E-06
-90.7	60.0	19540.5	8.22E-07

-----



	Transmitter	Primary Receiver	Secondary Receiver
Antenna Gain (dBi)	47.36	47.36	47.36
Line & Equip Loss (dB)	15.18	13.80	12.03
Frequency (GHz)		8.20	8.20
Polarization		Horizontal	Horizontal

Combined Multipath and Rain Loss Variability  
for the Path from FELDBERG  
Tower 0 to LANGERKOPF Tower 1

Figure 5-3. Time availability of received signal level.

## PROGRAM NO. 6, LINK PERFORMANCE CALCULATIONS

The purpose of the link performance program is to calculate the reliability and quality of a line-of-sight link used in either an analog or digital system. Performance must be evaluated for both long- and short-term services. For analog systems, long-term service quality is primarily a function of equipment quality and median signal level. This service quality is conveniently calculated using the computer (see Figure 6-1). For practical digital systems transferring data at rates less than 50 Mb/s, the long-term service quality is primarily a function of equipment quality. The median signal level required for optimum digital system quality is many dB less than that required for optimum analog quality (Bell Telephone Labs, 1970, pp. 553-554). This characteristic of digital systems with their nonmultiplicative noise build-up makes it unnecessary to calculate the long-term, high signal level quality of such systems. Short-term reliability and quality of both analog and digital systems are dependent on the propagation characteristics of the radio path. Calculation of short-term radio propagation reliability for a given value of signal quality is easily done using the desk-top computer system and is indicated in Figure 6-1.

Noise calculations for analog systems have not changed significantly in the past several years and the model presented here is much the same as the one used in MIL-HDBK-416 (1977).

To obtain an overall summary tabulation having link performance compared to applicable standards, the following steps are necessary:

1. Calculate standards requirements for FM-FDM links.
2. Obtain standards requirements for digital links.
3. Calculate the FM-FDM link, worst-channel receiver transfer characteristic (signal-to-noise ratio as a function of received-signal-level,  $P_r$ ). Thermal noise, equipment intermodulation distortion and feeder echo distortion must be calculated first to obtain the receiver transfer characteristic.
4. Calculate the digital link receiver transfer characteristic (bit-error-rate as a function of  $P_r$ ).

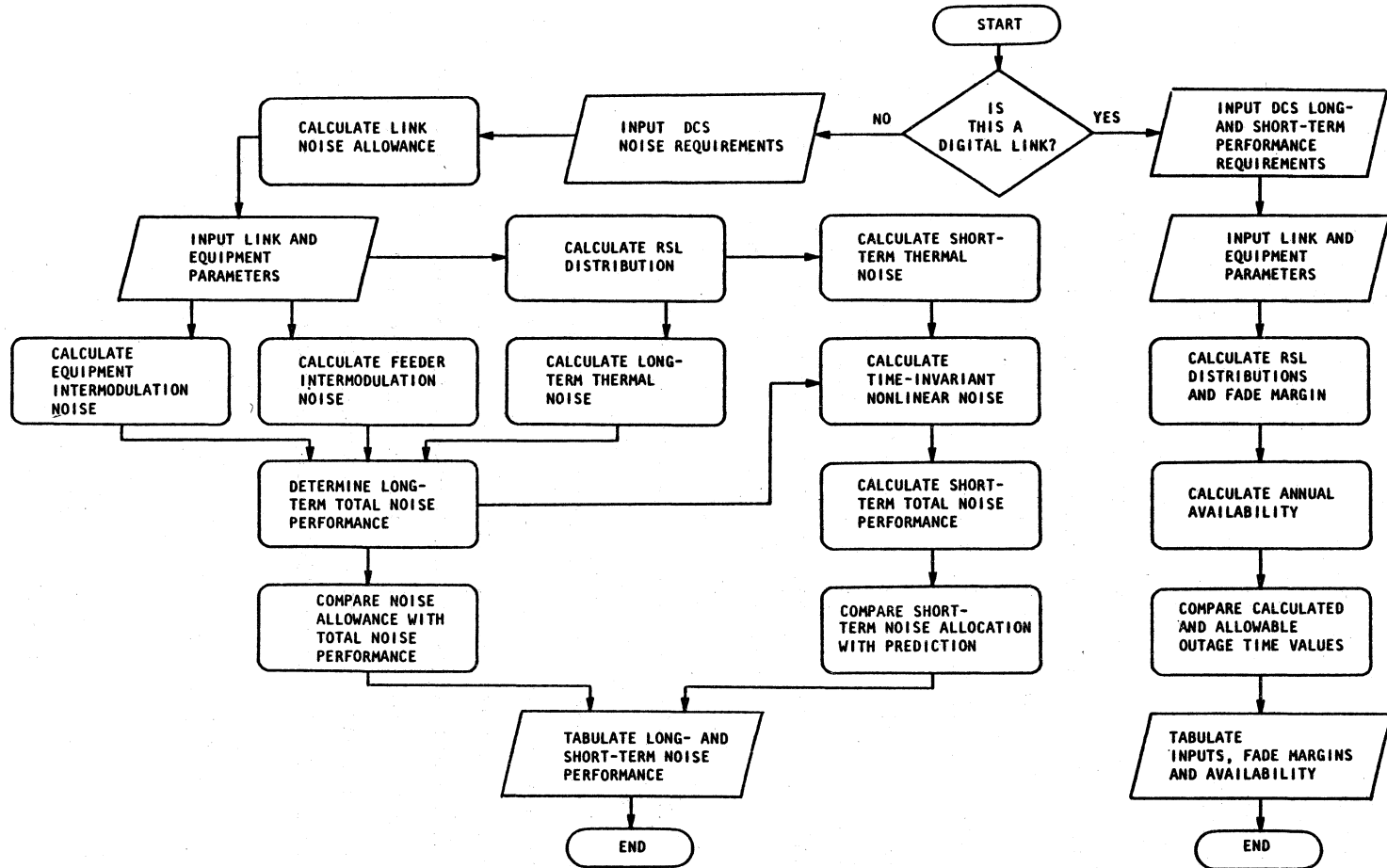


Figure 6-1. Link performance evaluation.

5. Calculate the outage time at the minimum allowable, short-term, signal quality level by comparing corresponding signal quality values from the receiver transfer characteristic with fraction of time values from the RSL time distribution (calculated in Program 5) using RSL as the comparison parameter.
6. Tabulate input variables, results from steps 1, 2, and 5 and other important information about the link.

Each of these steps will be discussed in the order shown above.

Defense Communications System (DCS) Noise Requirements for FM-FDM System Link Design:

On the basis of a hypothetical reference circuit, MIL-STD-188-300 (1971) in paragraph 4.3.3.1.2 allocates a maximum of 3.33 pWp0/km median noise level in the noisiest voice channel due to radio equipment and propagation. This value translates to approximately 3.2 pW0/km (flat weighting). In order to provide a design objective this value was selected as a standard of analog link quality comparison for Program No. 6. The 3.2 pW0/km value seems to be consistent with CCIR (1974b) and industry standards for high performance links (Broadhage and Hormuth, 1968, page 22). Most of this noise allocation is assigned to equipment noise since thermal noise is a small component at the median signal level. Median path length in terrestrial LOS microwave systems is approximately 35 km. Because of equipment noise predominance and the 35 km average distance, we can allocate an average of 112 pW0 of noise in the worst channel per link. For a specific combination of paths, a different link noise allowance may be calculated:

$$P_{NA} = \frac{3.2}{n} \sum_{i=1}^{i=n} d_i \quad (6-1)$$

where

$P_{NA}$  is the noise allowance per link in pW0.

$d_i$  is a path length in km.

$n$  is the number of paths.

$P_{NA} = 112$  pW0 is the default value of noise allowance per link.

It should not be cause for alarm if an individual link's median noise level does not fall within its assigned noise allowance since it is the summation of the median noise values which is important. (See Program No. 7.)

For short-term performance considerations, the maximum allowable flat weighted noise is 500,000 pW0 in the worst channel (MIL-STD-188-300, 1971, p. 48). 500,000 pW0 corresponds to a value of signal-to-noise ratio in the worst channel equal to 33 dB.

The signal-to-noise ratio is allowed to fall below 33 dB for no more than 10 minutes per year (approximately 2 min during the worst month, MIL-HDBK-416, 1977, p. 4-261) which is equivalent to an average availability of 0.99998 of the year.

DCS Short-Term Requirements for a Digital System Link Design:

MIL-STD-188-322 (1976) states that for LOS digital microwave systems: "It is a design objective to have a 30 dB minimum fade margin on all paths. All radio links are required to have a minimum annual path availability of 0.99995 for maintaining a bit error rate of  $5 \times 10^{-9}$  for operation below 10 GHz. All radio links are also required to have a minimum annual path availability of 0.99998 for maintaining a bit error rate of  $1 \times 10^{-2}$ ."

These availability values are the short-term requirements for digital systems. Long-term or median path performance (for error rates substantially less than  $5 \times 10^{-9}$ ) are not meaningful since such low error rates are generally a function of equipment performance, not path performance.

Long-Term (Median) Thermal Noise Calculation:

For purposes of system noise calculations, thermal noise is defined as noise from all sources in a channel when there is no modulated signal present on any of the channels in the microwave system. By this definition, thermal noise includes atmospheric and cosmic noise, and all intrinsic and thermal noise produced in the equipment when no modulation is present. Thermal noise is measured in a channel with all modulation removed from all channels of the system.

The signal-to-thermal noise ratio in an FDM-FM system is related to path loss variability. As the path loss on a hop becomes low, i.e., the

received signal level becomes high, the thermal noise is relatively quite low. As received signal level decreases toward FM threshold, the thermal noise becomes higher. Signal-to-thermal noise ratio,  $S/N_t$ , in a voice channel is proportional to received signal level,  $P_r$ , or carrier-to-noise ratio  $C/N$ . In the region above FM threshold,  $S/N_t$  may be expressed in several forms:

$$S/N_t = P_r + 20 \log \frac{\delta f}{f_m} - 10 \log (kTb_c \times 10^3) - F \quad (6-2)$$

$$S/N_t = P_r + 20 \log \frac{\Delta F}{f_m} - PF - LF - 10 \log (kTb_c \times 10^3) - F \quad (6-3)$$

$$S/N_t = C/N + 20 \log \frac{\Delta F}{f_m} - PF - LF + 10 \log \frac{B_{IF}}{b_c} \quad (6-4)$$

$$S/N_t = C/N + 20 \log \frac{\delta f}{f_m} + 10 \log \frac{B_{IF}}{b_c} \quad (6-5)$$

$$B_{IF} = 2 (\Delta F + f_m) \quad (6-6)$$

$$\Delta F = (\delta f) \left( \text{antilog} \frac{PF}{20} \right) \left( \text{antilog} \frac{LF}{20} \right) \text{ in kHz} \quad (6-7)$$

$$LF = -10 + 10 \log n \text{ in dB.} \quad (6-8)$$

$\Delta F$  is the peak carrier deviation in kHz

$\delta f$  is the rms per channel deviation in kHz

$S/N_t$  is the voice-channel-signal-to-thermal-noise ratio in dB

$P_r$  is the received carrier level in dBm,

$C/N$  is the predetection carrier-to-noise ratio in dB and  $N$  is the receiver front end thermal noise power in the same units as  $P_r$

$PF$  is the baseband signal peak factor of 13.5 dB

$LF$  is the RMS noise load factor in dB

$b_c$  is the usable voice channel bandwidth taken to be 3.100 kHz

$B_{IF}$  is the receiver IF bandwidth in kHz

$f_m$  is the highest modulating frequency in the baseband in kHz

$F$  is the receiver noise figure in dB

$k$  is Boltzman's constant,  $1.3804 \times 10^{-20}$  millijoules/degree K

$T$  is the antenna temperature taken to be 290 degrees K, and

$n$  is the number of voice channels in the baseband.

The value of  $P_r$  at which thermal noise threshold,  $P_r(\text{TH})$ , occurs is given by the equation:

$$P_r(\text{TH}) = 30 + 10 \log (kTB_{\text{IF}} \times 10^3) + F. \quad (6-9)$$

The value of  $P_r$  at which FM threshold occurs,  $P_r(\text{FMTH})$ , is:

$$P_r(\text{FMTH}) = 10 + P_r(\text{TH}). \quad (6-10)$$

The terms on the right-hand side of equations 6-2 and 6-3 with the exception of  $P_r$  may be calculated for a given set of equipment parameters. This then becomes a constant - a figure of merit - and as  $P_r$  is allowed to vary, the voice channel signal-to-thermal-noise ratio varies in proportion. Using this information, a receiver thermal noise transfer characteristic or "quieting curve" may be constructed, where its slope is uniquely determined by any of the above equations for conditions above FM threshold.

#### Equipment Intermodulation Noise Calculation:

Equipment intermodulation noise, for the purpose of system noise calculations, is defined as the total noise from all sources produced as a result of the presence of a modulated signal in the system except feeder echo noise. Intermodulation noise is measured in a channel with all modulation removed from the channel being measured, and with all remaining channels loaded with actual traffic or with an equivalent amount of white (randomly-distributed) noise over a specific bandwidth. The intermodulation noise power in the channel is then equal to the measured total noise with modulation present, less the measured thermal noise with no modulation present.

The values of noise power ratio (NPR) in the channel having the worst signal-to-noise ratio must be obtained from either equipment performance specifications or carefully controlled tests. The specific loading conditions and received signal level (RSL) must be known for each NPR value. Of particular importance, is the NPR value corresponding to the optimum RSL for a particular microwave radio.

If information is not available, an NPR value of 55 dB obtainable using new, quality equipment is probably the highest value that can be

assumed for the initial estimate. A pre-emphasis improvement of 4 dB in the worst channel is usually assumed included in this NPR value.

The above discussions hold for remodulating (baseband) radios. If the designer is concerned with heterodyne repeaters, the above measurements become very difficult to make and the designer has to rely on manufacturers' specifications. Alternatively, a 4 dB improvement in NPR (Lenkurt Electric Co., 1970) over the remodulating radio may be assumed. For example, if a 55 dB NPR is assumed for the remodulating radio, a 59 dB NPR would be used for a similar quality heterodyne unit.

Allocation of calculated noise is difficult particularly for mixed systems on a hop; i.e., a remodulating transmitter at one end and a heterodyne repeater receiver at the other end. Very little information exists on the noise contribution of the individual components or even that of the transmitter and receiver separately. For an engineering estimate, the equipment intermodulation noise may be allocated in equal parts to the transmitter side and the receiver side.

The noise power ratio can now be converted to an equivalent noise channel signal-to-equipment intermodulation noise ratio,  $S/Ne$ , and additionally to equipment intermodulation noise,  $Ne$ :

$$S/Ne = NPR + 10 \log (B_b/b_c) - LF \text{ dB} \quad (6-11)$$

$$Ne = \text{antilog} \frac{90 - S/Ne}{10} \text{ pW0} \quad (6-12)$$

$$B_b = f_m - f_\ell \quad (6-13)$$

where

$f_m$  = the upper baseband frequency (kHz).

$f_\ell$  = the lower baseband frequency (kHz).

$b_c$  = the nominal voice channel bandwidth, 3.100 kHz.

LF = the RMS load factor in dB (see eq. 6-8).

In these noise calculations flat-weighted noise will be used for ease in handling. If the designer desires to use other noise weightings, appropriate factors may be included at the conclusion of the design procedure.

### Feeder Intermodulation Noise Calculation:

If a transmission line many wavelengths long is mismatched at both the generator and load ends, its frequency-phase response is linear with a small sinusoidal ripple, and this leads to reflected waves in the line that cause distortion of an FM signal. This type of distortion is more conveniently considered as being caused by an echo signal generated in a mismatched line, which results in intermodulation distortion. Significant levels of this type of intermodulation noise are reached when the waveguide lengths exceed approximately 20 meters per individual antenna, or 30 meters total per hop (MIL-HDBK-416, 1977, p. 4-284).

The feeder intermodulation noise is also considered to be independent of path loss or signal level variations and is therefore another component of the time invariant nonlinear noise power.

Feeder intermodulation noise,  $N_f$ , may be approximated given transmission line lengths, velocity of propagation in the lines, transmission system component VSWR's or return losses, transmission line losses and directional losses. The calculations are performed separately for each end of a hop; i.e., transmitter and receiver, and the results are summed to determine the total hop contribution.

To calculate  $N_f$  in the worst channel, the echo delay time is first calculated. Determine echo delay time,  $\tau$ , from the transmission line length,  $L$ , and the percent velocity of propagation, ( $\% v$ ), obtained from Figure 6-2 using:

$$\tau = 2L/V \text{ s, where } V = (3 \times 10^8) (\% v \times 10^{-2}) \text{ m/s.} \quad (6-14)$$

Reasonable default values for  $V$  are:

$$V = 0.65 (3 \times 10^8) \text{ for elliptical waveguide and}$$

$$V = 0.75 (3 \times 10^8) \text{ for rectangular waveguide.}$$

The echo delay time is then converted to radian delay,  $\theta_o$ :

$$\theta_o = 2\pi f_m \tau \times 10^3 \quad (6-15)$$

where  $f_m$  is the highest modulating frequency in the baseband. The echo power,  $r$ , relative to the signal power causing it is given by the expression:

$$r = RL_e + RL_a + 2A_{tl} \quad (\text{MIL-HDBK-416, 1977, pp. 4-286, 4-389}) \quad (6-16)$$

Courtesy of Dr. John Osepchuk (MIL-HDBK-416, 1977).

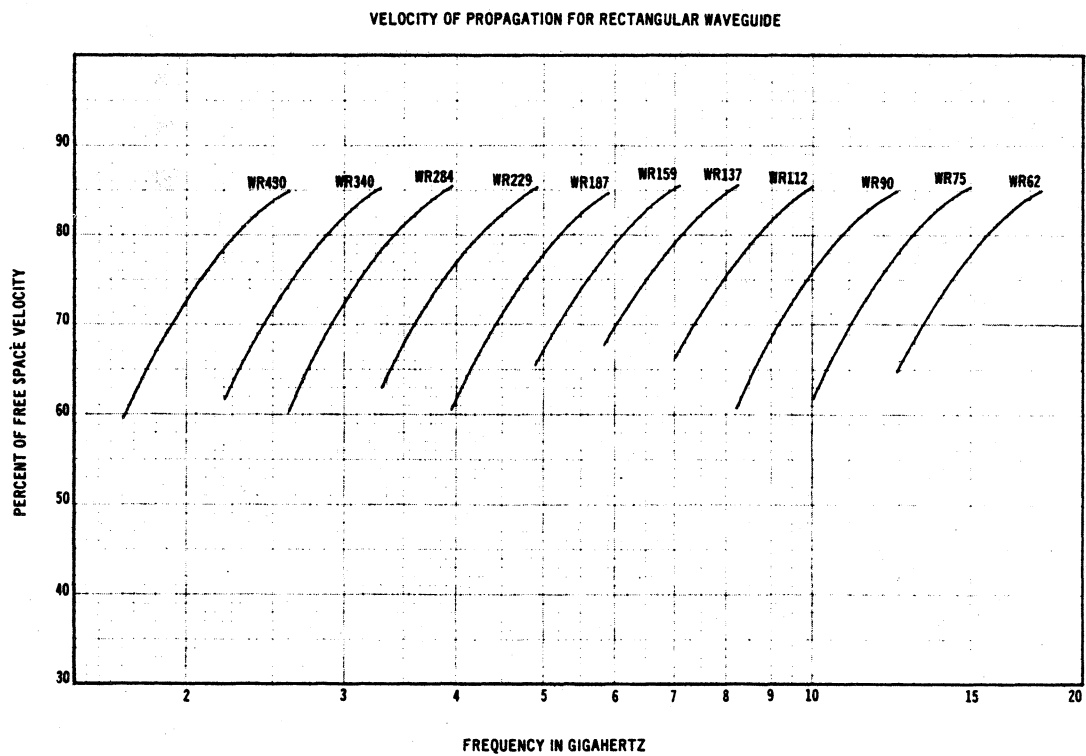
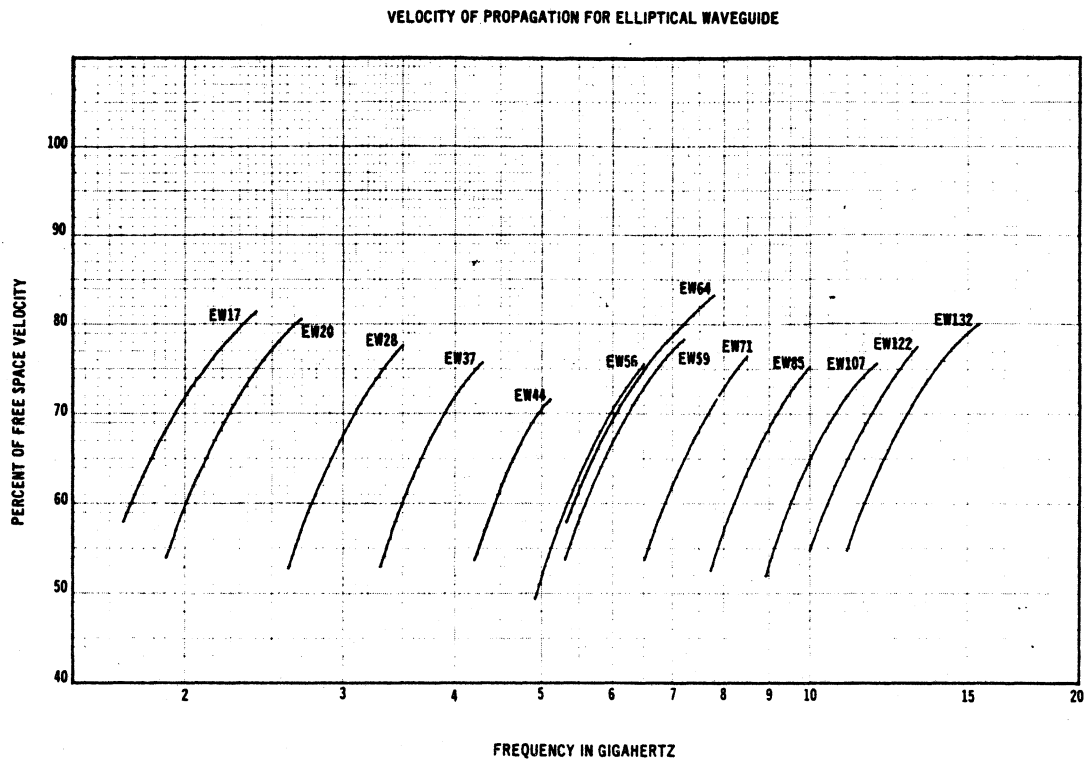


Figure 6-2. Waveguide velocity curves.

where  $r$  = the number of dB that the echo is down from the signal power

$A_{tl}$  = the transmission line loss in dB.

$RL_e$  = the return loss (dB) at the interface between the transmission line and either the transmitter or receiver (whichever case is applicable).

$RL_a$  = the return loss (dB) at the interface between the transmission line and the antenna.

This model assumes that all discontinuities are negligible with respect to the ones at these interfaces in the intermediate section of the transmission line between the transmitter or receiver and the antenna.

If parameters other than return loss are provided such as the VSWR or the voltage reflection coefficient,  $\rho$ , they can be converted to return loss, RL, using the following expressions:

$$\rho = \frac{VSWR - 1}{VSWR + 1} \quad (6-17)$$

$$RL = 20 \log (1/\rho). \quad (6-18)$$

The power in the echo cannot totally be considered as distortion power,  $D$ , unless the echo delay is large. To obtain the value of  $S/D$ , a "parameter A" must be determined:

$$A = \frac{\delta f}{f_m} \times 10^{\frac{LF}{20}} \quad (6-19)$$

or alternatively,

$$A = \frac{\delta f}{f_m} \left( \frac{n}{10} \right)^{1/2}. \quad (6-20)$$

(The variables in the equations for A have been defined earlier in this section. See equation (7-8) to calculate LF.)

Using parameter A and  $\theta_o$ ,  $(\frac{S}{D} - r)$  can now be obtained from Figure 6-3) A good approximation (developed by the authors) for  $\frac{S}{D} - r$  can be obtained from the equations:

$$F_1(A, \theta) = 7.17 - 8.23 \ln A + 40 \log \frac{1}{\theta} \quad (6-21)$$

$$F_2(A) = 9.421 - 54.84A + 113.2A^2 - 88.5A^3 + 31.52A^4 - 4.239A^5 \quad (6-22)$$

where  $\frac{S}{D} - r$  equals the greater of  $F_1$  and  $F_2$ .

SIGNAL/DISTORTION MINUS ECHO AMPLITUDE, S/D-r, dB

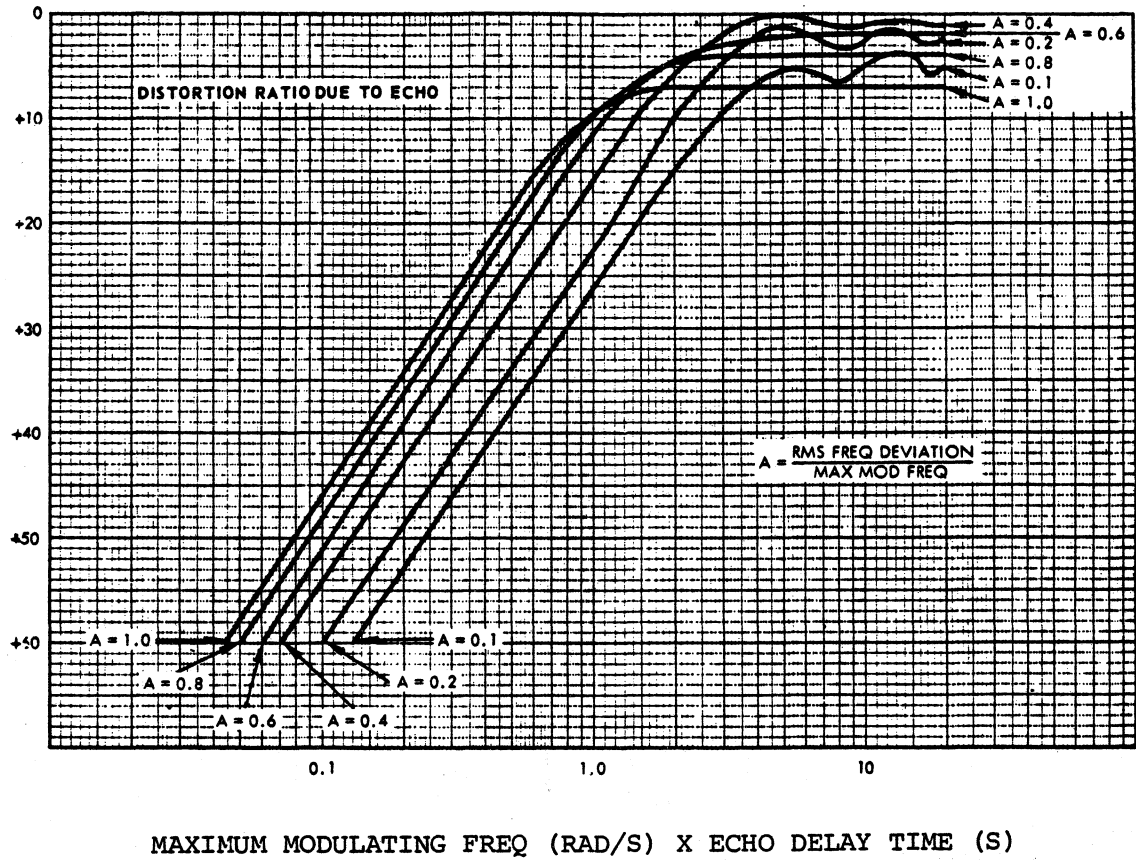


Figure 6-3. Maximum distortion to signal ratio due to echo.

The calculation of echo attenuation (separately for transmitter and receiver) outlined above can now be converted to voice channel noise. To do this, the total echo attenuation,  $r$ , is added to the  $(S/D - r)$  value obtained from Figure 6-3.

This results in the signal-to-distortion ratio,  $S/D$  which must be corrected for the ratio of baseband to voice channel bandwidth and for the RMS load factor. In equation form, the voice channel signal to feeder echo noise ratio becomes:

$$S/N_f = S/D + 10 \log \frac{B_b}{b_c} - LF \text{ dB.} \quad (6-23)$$

The conversion to flat-weighted noise is as follows:

$$N_f = \text{antilog} \frac{90 - S/N_f}{10} \text{ pW0.} \quad (6-24)$$

The foregoing feeder echo noise calculations are performed separately for each end of a hop by arbitrarily designating one end the transmitter and the other end the receiver. At the conclusion, these two noise results are summed together to give a total hop feeder echo noise contribution.

The sum of the total feeder echo noise and equipment intermodulation noise in this design will be called the time invariant nonlinear noise since these noise components do not depend on path loss variability. This total noise component is normally the dominant contribution for relatively high signal levels near the long-term median.

The effect of using a linear adder or maximal ratio combiner is to decrease the time invariant nonlinear noise ( $N_e + N_f$ ) in all channels by a factor of 1/2. This combiner improvement,  $I_c$ , is approximately 3 dB or 0 dB depending on the combiner type.

#### Pre-Emphasis/De-Emphasis:

As a result of the linear frequency modulation process, channel noise power increases with baseband frequency so that the higher channels have smaller signal-to-noise ratios than the lower ones. To compensate for this effect in most radio-relay systems, pre-emphasis is applied. Pre-emphasis means that before frequency modulation is accomplished in

the transmitter the level of the upper part of the baseband is increased while the level of the lower part is decreased. This is done in a manner such that the mean total baseband power is the same as it was before pre-emphasis was applied. The result is that noise in the channels is redistributed so that the  $S/N_T$  in the worst channel is improved at the expense of the better channels. In the worst channel, pre-emphasis/de-emphasis improvement,  $I_p$  is approximately 4 dB if the CCIR network is used (EIA Standard, 1972, pp. 30-34).

Receiver Transfer Characteristic for FM-FDM Systems:

The receiver transfer characteristic is one of the outputs of Program No. 6 (Figure 6-4). The receiver transfer characteristic is called the quieting curve when feeder echo noise is not included in its calculation. This transfer curve is a good indication of the link dynamic performance characteristics. It is essentially a plot of worst voice channel signal-to-noise in decibels as a function of received signal level. The receiver transfer characteristic is limited at the upper end (high received signal levels) by the equipment intermodulation noise, and at the lower end by the FM improvement threshold.

The available dynamic range for linear system performance is that portion of the unity-slope straight line between the FM improvement threshold and the line intersection with the  $S/(N_e + N_f)$ .

Performance below the FM improvement threshold can be approximated by a line with a slope of 4 (4 dB decrease in signal-to-noise ratio for each 1 dB decrease in received signal level) at S/N values lower than that corresponding to the FM improvement threshold.

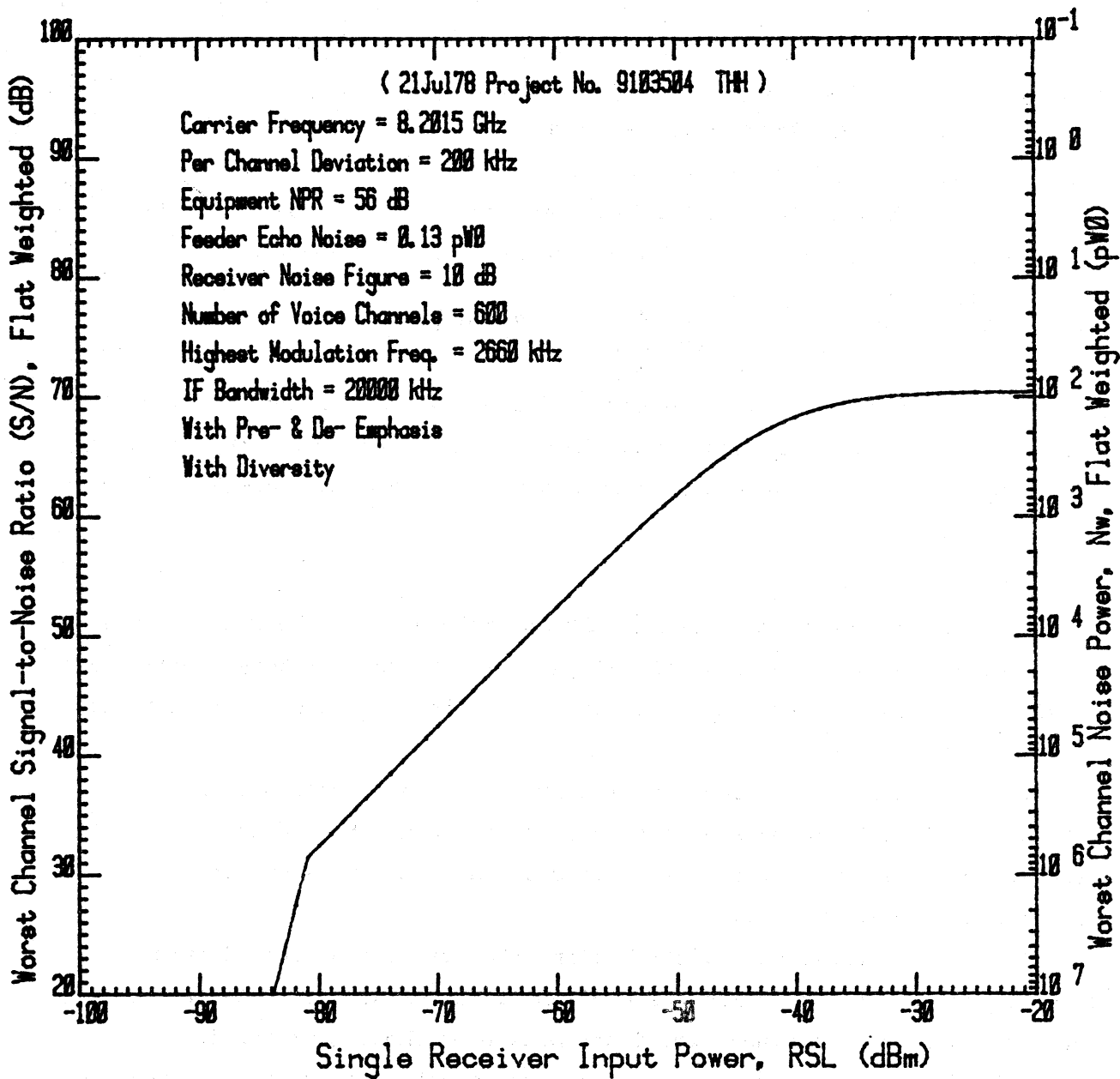
The equation for the receiver transfer characteristic includes feeder echo noise as well as thermal noise and equipment noise. For performance above FM threshold, worst channel signal-to-noise ratio,  $S/N_w$ , is given by the equation:

$$S/N_w = 90 - 10 \log N_w \tag{6-25}$$

where  $N_w$  is the noise in the worst channel

$$N_w = (\text{antilog } (-I_p/10) (N_T) + \text{antilog } (-I_p/10) (N_e + N_f)). \tag{6-26}$$

See equation 6-10 to calculate the value of  $P_r$  at which FM threshold occurs.



FM/FDM Equipment Transfer Characteristic  
 For the Link from FELDBERG Tower Ø  
 To LANGERKOPF Tower 1

Figure 6-4. Example of a worst channel FM-FDM receiver transfer characteristic.

### Receiver Transfer Characteristic for Digital Systems:

Although the bit-error-rate, BER, threshold will vary for various types of digital receivers, the shape of the transfer characteristic will generally remain the same in the presence of Gaussian noise (Bell Telephone Labs., 1970, p. 629). The equation for the receiver transfer characteristic is:

$$\text{BER} = \frac{1}{2} \operatorname{erfc} \left( k_o \times 10^{P_r/20} \right) \quad (6-27)$$

where the constant,  $k_o$ , may be determined from the BER threshold using a successive approximation method described in a book by G.E. Forsythe, et al., (1977 pp. 161-165). Figure 6-5 is an example of a digital receiver transfer characteristic.

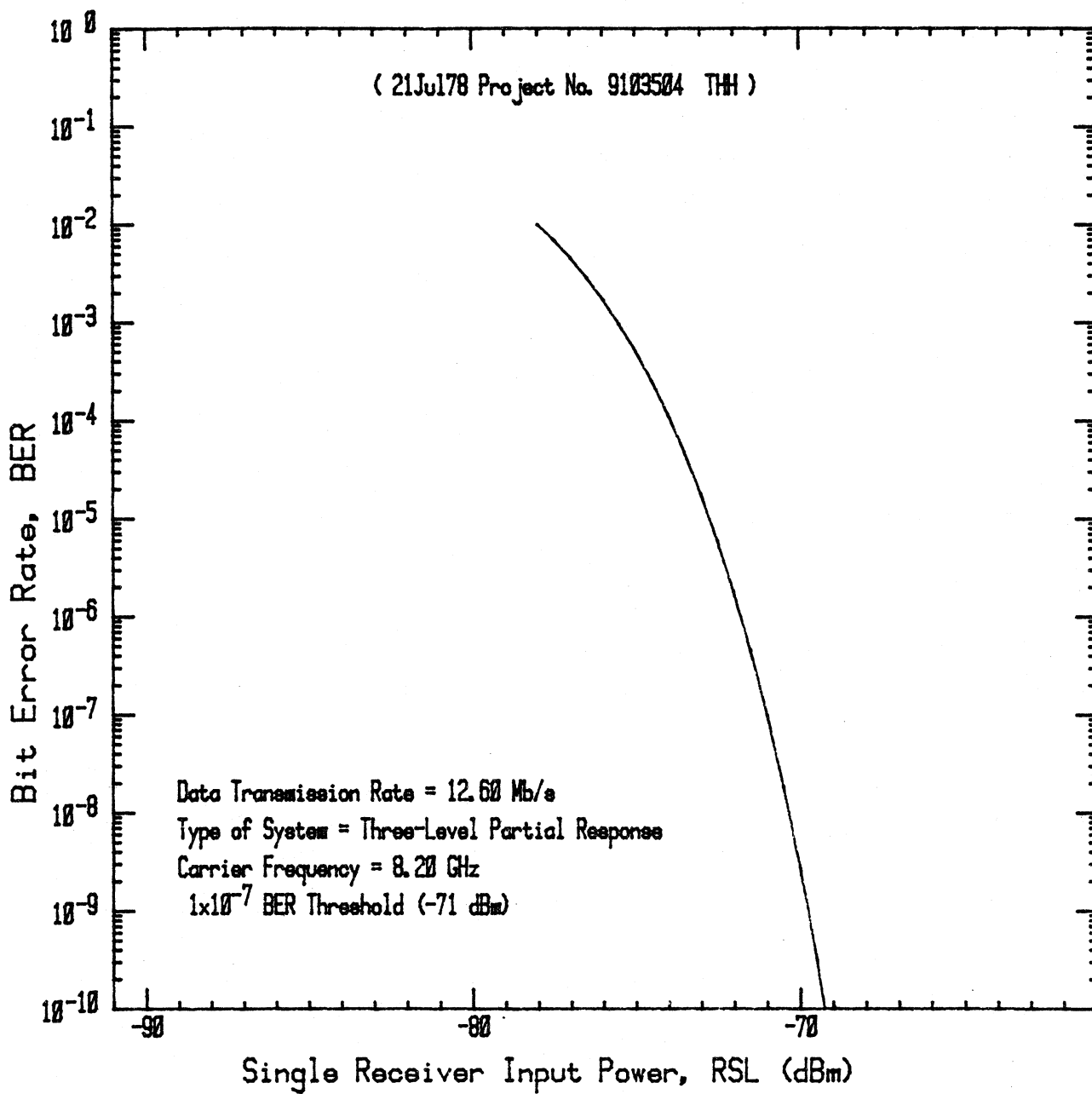
### Outage Time Calculations:

Using either maximum allowable BER or maximum allowable worst channel noise power, the minimum value of RSL suitable for satisfactory short-term service is calculated from the appropriate receiver transfer characteristic described above.

In Program No. 5, a combined time distribution of multipath and rain attenuation is calculated and this function is then fitted using straight line approximations between a few points so that it may be carried conveniently to Program No. 6.

From the combined time distribution, the fraction of annual outage time is then calculated using the minimum values of RSL for satisfactory service. When the combined time distribution of short-term RSL is primarily due to rain attenuation, one more important piece of information is desirable. This information is how often the calculated short-term outage RSL level will occur. Will it occur twice per year or once every two years, etc? As desirable as this information would be, a reasonably reliable model is not available in the literature at this time. Lin (1977) p. 1589, does, however, point out that the annual outage time of a radio route is statistically more stable than that of a radio link which indicates that this type of information is not so important as it first appears to be.

All that remains to be done on the link analysis is to tabulate the link performance summary. Table 6-1 is an example of this summary.



PCM-TDM Equipment Transfer Characteristic  
 For the Link from FELDBERG Tower 0  
 To LANGERKOPF Tower 1

Figure 6-5. Example of a digital receiver transfer characteristic.

Table 6-1. Example of the Link Performance Summary

Design Summary for the FM/FDM Link  
from FELDBERG to LANGERKOPF (Sheet 1)

(21Jul78 Project No. 9103504 THH)

Input Parameters:

System Type	=	FM/FDM
Path Length	( km) =	114.55
Polarization	=	Vertical
Mean Path Temperature	(C) =	20
Mean Path Pressure	(kPa) =	94
Absolute Humidity	(gm/cu. m) =	12
Average Path Height Above Ground	(m) =	321
Terrain Type	=	Mountains
Mean Annual Rainfall	(mm) =	800
Mean Thunderstorm Ratio	=	0.25
Annual No. of Rainy Days	=	100
Receiver Front-End Type	=	20DBPREAMP
Receiver Front-End Location	=	ANTENNA
Diversity Configuration	=	DUAL SPACE
Combiner Location	=	PRE DETEC
Combiner Type	=	MAX RATIO

Table 6-1. Example of the Link Performance Summary (con't)

Design Summary for the FM/FDM Link  
 from FELDBERG to LANGERKOPF (Sheet 2)

<u>Input Parameter</u>	<u>Transmitter</u>	<u>Receiver</u>	
		<u>Primary</u>	<u>Secondary</u>
Site Designator	= FEL		LKF
Tower Number	= 0		1
Latitude	= 50 14'33.00"N	49 18' 4.00"N	
Longitude	= 8 29'49.00"E	7 50'47.00"E	
Tower Base Elev. above MSL (m)	= 688.80	602.00	
Azimuth from True north	=204 18' 1.69"	23 48'13.55"	
Azimuth from Magnetic North	=192 15'	11 41'	
Antenna Height above Ground (m)	= 120.00	105.00	90.00
Antenna Type	= PARABOLIC	PARABOLIC	PARABOLIC
Antenna Gain (dBi)	= 47.36	47.36	47.36
Antenna Diameter (m)	= 3.66	3.66	3.66
Feeder Type	= EW85	EW85	EW85
Feeder Loss (dB/100m)	= 10.50	10.50	10.50
Feeder Length (m)	= 140.00	125.00	110.00
Total Line Loss (m)	= 14.70	13.13	11.55
Circulator/Diplexer Loss (dB)	= 1.00	1.00	1.00
Feeder Velocity Ratio	= 0.61	0.61	0.61
VSWR at Antenna	= 1.06	1.06	1.06
Return Loss at Antenna (dB)	= 30.71	30.71	30.71
VSWR at Radio	= 1.06	1.06	1.06
Return Loss at Radio (dB)	= 30.71	30.71	30.71

Table 6-1. Example of the Link Performance Summary (con't)

Design Summary for the FM/FDM Link  
from FELDBERG to LANGERKOPF (Sheet 3)

Parameter	Value
Primary Carrier Frequency (GHz)=	8.20
Secondary Carrier Frequency (GHz)=	
Transmitter Power (dBm)=	43.00
Transmitter Antenna Gain (dBi)=	47.36
Primary Receiver Antenna Gain (dBi)=	47.36
Second Receiver Antenna Gain (dBi)=	47.36
Transmitter Line Loss (dB)=	14.70
Primary Receiver Line Loss (dB)=	13.13
Second Receiver Line Loss (dB)=	11.55
Median Basic Trans. Loss (dB)=	
Expected Median RSL - Recv P (dBm)=	-29.89
Expected Median RSL - Recv S (dBm)=	-29.89

Table 6-1. Example of the Link Performance Summary (con't)

Design Summary for the FM/FDM Link  
from FELDBERG to LANGERKOPF (Sheet 4)

Parameter	Value
Is Pre & De-Emphasis Used ?	Yes
Number of 3.1 kHz Channels	= 600
Receiver IF 3dB Bandwidth	(kHz)= 20000.00
Equipment NPR	(dB)= 56.00
Peak Carrier Deviation	(kHz)= 7330.03
RMS per Channel Deviation	(kHz)= 200.00
Receiver Noise Figure	(dB)= 10.00
FM Threshold	(dBm) = -80.97
Baseband Signal Peak Factor	(dB)= 13.5
RMS Noise Load Factor	(dB)= 17.78
Voice Channel Bandwidth	(kHz)= 3.1
Highest Mod. Freq. in BB	(kHz)= 2660.00
Thermal Noise at Median RSL	(pW0) = 14.03
Feeder Echo Noise	(pW0) = 0.13
Equipment Noise	(pW0) = 179.70
Total Long-Term Noise	(pW0) = 95.71
Long Term Noise Allowance	(pW0) = 112.00
Desired Availability	= 0.99998
Calculated Availability	= 0.99995
Fade Margin	(dB)= 45.52

Table 6-1. Example of the Link Performance Summary (con't)

Design Summary for the PCM/TDM Link

from FELDBERG to LANGERKOPF (Sheet 4, alternate printout for digital systems)

Parameter	Value
Data Transmission Rate	(Mb/s) = 12.60
RSL at BER Threshold	(dBm) = -71.00
BER at BER Threshold	= 1.00E-07
Desired Availability	= 0.99995
at BER	= 1.00E-09
Calculated Availability	= 0.99990
at BER	= 1.00E-09
Fade Margin	(dB) = 39.87

## PROGRAM NO. 7, SYSTEM PERFORMANCE

The main purpose of the System Performance Program is to provide in tabular form a summary showing long- and short-term system performance for a number of tandem links. The flow diagram for the system performance evaluation model is presented in Figure 7-1.

Tables 7-1 and 7-2 are example tabulations for an FM/FDM and a digital system, respectively. The tabulations can be used as an aid in deciding which links should have their requirements relaxed or tightened. By means of this iterative process, an optimum design may then be calculated. Tables 7-1 and 7-2 are for links going in one direction from one end of the system to the other. Obviously, a pair of tables is required for each system. One table is needed for links from east to west and the other from west to east. The allocated system noise is obtained by multiplying  $3.2 \text{ pW0}$  and the total length of the system in kilometers (see eq. 6-1). Computed system availability is obtained by multiplying the values of availability for each path. Allocated system outage time is obtained by dividing the system length by the average path length (35 km) and multiplying that ratio and the allowable link outage time, 0.00002, (MIL-STD-188-322, Table 1). This outage time subtracted from 1 gives the allocated system availability.

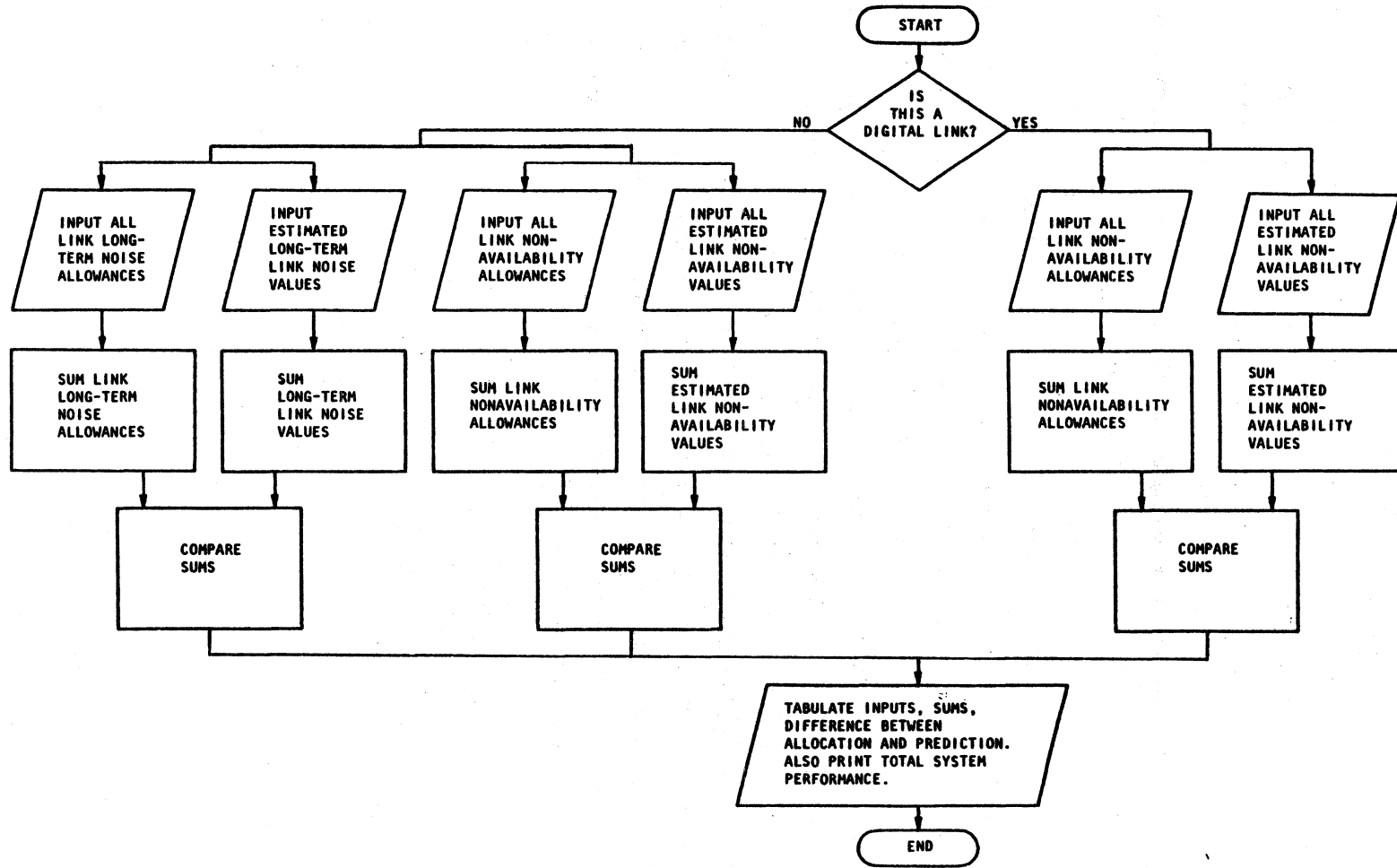


Figure 7-1. System performance evaluation.

Table 7-1. Example FM/FDM System Performance Table

Performance Prediction for the FEL-RHN FM/FDM System

(26Sep78 Project No. 9103504 LGH)

Link	Freq. (GHz)	Path Length (km)	Fade Margin (dB)	Computed Noise (pW0)	Allocated Noise (pW0)	Computed Avail.	Allocated Avail.
FEL-LKF	8.2015	114.55	45.52	96	112	0.999952	0.999980
LKF-RHN	8.7500	57.60	44.10	151	112	0.999960	0.999980
<b>System Values:</b>		<b>172.15</b>		<b>247</b>	<b>551</b>	<b>0.999912</b>	<b>0.999902</b>

Table 7-2. Example Digital System Performance Table

Performance Prediction for the FEL-RHN Digital System  
(26Sep78 Project No. 9103504 LGH)

Link	Freq. (GHz)	Path Length (km)	Fade Margin (dB)	Computed Avail.	Allocated Avail.
FEL-LKF	8.2015	114.55	45.52	0.999952	0.999980
LKF-RHN	8.7500	57.60	44.10	0.999960	0.999980
System Values:		172.15		0.999912	0.999902

## 8. RECOMMENDATIONS

The seven microwave system design programs described in this report go far in reducing the cost of designing a microwave line-of-sight system but there are many other labor intensive tasks which would be done better and at less cost than they are now done by using interactively programmed desk-top computers. Some of these tasks are listed below:

1. Design of passive repeater systems.
2. Design of obstacle diffraction paths.
3. Reading of detailed map profiles onto disc memory by using the map following, reading and digitizing capabilities of modern microprocessor controlled plotters.

In addition to the design of systems, record keeping capabilities of desk-top computer systems are very efficient in the use of time and space since, in many instances, an ordinary notebook full of flexible discs can hold more information than a file cabinet. The indices and contents of discs can conveniently and quickly be displayed or produced in hard copy. These discs are readily kept current. Such things as site layout and tower stress diagrams can be stored as well as daily site or system logs and maintenance records. These concepts are practical provided that interactive programs are developed which guide the user and are convenient to operate. It is recommended that these capabilities be considered and compared with present on-site record keeping methods.

The seven programs that have been developed can be much improved in the light of continued user experience and new improvements in the models on which they are based. It is recommended that a continuing effort be made to improve the programs and that periodically the models themselves be carefully re-examined as a result of improvements reported in the open literature. This statement is particularly true of the rain attenuation, multipath, and digital link and system performance models which are in a state of rapid development.

## 9. . REFERENCES

- Andrew Corp, (1978), Antenna Systems, Catalog 30, 151.
- The American Ephemeris and Nautical Almanac for the Year 1975 (1973),  
Nautical Almanac Office U.S. Naval Observatory, Superintendent of  
Documents, U.S. Government Printing Office, Washington, D.C. 20402.
- Barnett, W.T. (1972), Multipath Propagation at 4, 6, and 11 Bell  
System Tech. J., Vol-51, No. 2, 321-361, Feb.
- Bell Telephone Laboratories (1970), Transmission Systems for Communica-  
tions (Western Electric Company, Inc., Winston-Salem, N.C.).
- Brodhage, H., and W. Hormuth (1968), 7th Ed., Planning and Engineering of  
Radio Relay Links, (Siemens Aktiengesellschaft, Munich, Germany).
- CCIR, (1974a), Doc. Vol 5, Geneva, Switzerland.
- CCIR, (1974b), Doc. Vol 9, Rec. 395-1, Geneva, Switzerland.
- Dutton, E.J., H.T. Dougherty, and R.F. Martin, Jr. (1974), Prediction of  
European rainfall and link performance coefficients at 8 to 30 GHz,  
Technical Report No. ACC-ACO-16-74, AD/A-000804.
- Dutton, E.J. (1977), Precipitation variability in the U.S.A. for microwave  
terrestrial system design, OT/ITS, OT Report 77-134.
- EIA, Electronic Industries Association (1972), Standard Microwave Transmis-  
sion Systems, EIA Std. RS-252-A, (Electronics Ind. Assoc., Engineering  
Dept., 2001 Eye Street, N.W., Washington, D.C. 20006).
- Forsythe, G.E., M.A. Malcolm, and C.B. Moler (1977), Computer Methods for  
Mathematical Computations, Prentice-Hall, Inc., Englewood Cliffs,  
NJ 07632.
- Hogg, D.C., A.J. Giger, A.C. Longton, and E.E. Muller (1977), The Influence  
of rain on design of 11-GHz terrestrial radio relay, Bell System  
Tech. J., Vol 56, No. 9.
- ITT, International Telephone and Telegraph Corporation (1975), Reference  
Data for Radio Engineers, H.P. Westman, ed., 6th edition (Howard W. Sams  
and Co., New York, N.Y.).
- Kamela, Czeslaw (1964), Dynamic Geodesy, Vol-1, (The Scientific Publica-  
tions Foreign Cooperation Center of the Central Institute for  
Scientific, Technical and Economic Information, Warsaw, Poland).
- Lenkurt Electric Company (1970), Engineering Considerations for Microwave  
Communications Systems, (GTE Lenkurt Dept. C134, San Carlos,  
California 94070).

- Liebe, H.J. and G.G. Gimmestad (1978), Calculation of clear air EHF refractivity, Radio Science, Vol 13, No. 2, March-April 1978.
- Lin, S.H. (1977), Nationwide long-term rain rate statistics and empirical calculation of 11 GHz microwave rain attenuation, Bell System Tech. J., Vol-56, No. 9.
- List, R.J. (1951), Smithsonian Meteorological Tables, 6th Ed., (Smithsonian Institution, Washington, D.C.).
- MIL-HDBK-416, Department of Defense (1977), Design Handbook for Line-of-Sight Microwave Communications System.
- MIL-STD-188-300, Department of Defense (1971), Standards for Long Haul Communications - System Design Standards Applicable to the Defense Communications Systems.
- MIL-STD-188-322, Department of Defense (1976), Subsystem Design/Engineering and Equipment Technical Design Standards for Long Haul Line-of-Sight (LOS) Digital Microwave Radio Transmission.
- Morita, Kazuo (1970), Prediction of Rayleigh fading occurrence probability of line-of-sight microwave links, Review of the Electrical Commun. Laboratory, Vol 18, Nos. 11-12, 810-822.
- Morris, D.E., C.J. Christopher, G.W. Chance, D.B. Barney (1976), Third Generation Programmable Calculator has computer-like capabilities, Hewlett-Packard Journal, Vol 27, No. 10.
- Rice, P.L. and N.R. Holmberg (1973), Cumulative Time Statistics of surface-point rainfall rates, IEEE Trans. on Comm., Vol. COM-21, No. 10.
- The Times Atlas of the World (1975), (Comprehensive Edition), Times Books in collaboration with John Bartholomew & Son Limited, Edinburg, Scotland.
- Vigants, A. (1975), Space-Diversity Engineering, Bell Systems Tech. J., Vol-54, No. 1, 103-142.

**BIBLIOGRAPHIC DATA SHEET**

1. PUBLICATION OR REPORT NO. NTIA Report 79-18		2. Gov't Accession No.	3. Recipient's Accession No.
4. TITLE AND SUBTITLE Automated digital system engineering model		5. Publication Date March 1979	6. Performing Organization Code NTIA/ITS
7. AUTHOR(S) L.G. Hause and D.R. Wortendyke		9. Project/Task/Work Unit No. 9101905	
8. PERFORMING ORGANIZATION NAME AND ADDRESS Department of Commerce National Telecommunications and Information Administration, Institute for Telecommunication Sciences Boulder, CO 80303		10. Contract/Grant No. CCC-PO-8-77	
11. Sponsoring Organization Name and Address U.S. Army Communications - Electronics Engineering Installation Agency Fort Huachuca, AZ 85613		12. Type of Report and Period Covered NTIA Report	
14. SUPPLEMENTARY NOTES		13.	
15. ABSTRACT (A 200-word or less factual summary of most significant information. If document includes a significant bibliography of literature survey, mention it here.) This report describes a desk-top computer system and mathematical models which were used in seven of its programs. These programs make key calculations in the design of line-of-sight microwave systems. The models have the following ranges; bit rates up to 50 Mbits/s, carrier frequencies from 1 to 40 GHz, and path distances up to 150 km. The programs calculate, tabulate and plot information about earth geometry, path profiles and ray paths, median basic transmission loss, path-loss variability, equipment gain, link performance, and system performance. Models were chosen based on their wideness of acceptance and the size and type of data base substantiating the model. Any design engineer using this model can have immediate access to calculated results corresponding to changes in design parameters. The reasons for this capability are that the programs are written for use in an interactive mode and the programs can be used by people with no experience in programming.			
16. Key works (Alphabetical order, separated by semicolons) Line-of-sight microwave, computer program, earth geometry, path profiles, basic transmission loss, digital systems, micromave link performance, multipath fading, rain attenuation			
17. AVAILABILITY STATEMENT <input checked="" type="checkbox"/> UNLIMITED. <input type="checkbox"/> FOR OFFICIAL DISTRIBUTION.		18. Security Class (This report) Unclassified	20. Number of pages 98
		19. Security Class (This page) Unclassified	21. Price:

